

Spectroscopy of neutron-rich  $^{34,35,36,37,38}\text{P}$  populated in binary grazing reactions

R. Chapman,<sup>1,\*</sup> A. Hodsdon,<sup>1</sup> M. Bouhelal,<sup>2</sup> F. Haas,<sup>3</sup> X. Liang,<sup>1</sup> F. Azaiez,<sup>4</sup> Z. M. Wang,<sup>1</sup> B. R. Behera,<sup>5</sup> M. Burns,<sup>1</sup> E. Caurier,<sup>3</sup> L. Corradi,<sup>5</sup> D. Curien,<sup>3</sup> A. N. Deacon,<sup>6</sup> Zs. Dombrádi,<sup>7</sup> E. Farnea,<sup>8</sup> E. Fioretto,<sup>5</sup> A. Gadea,<sup>5</sup> F. Ibrahim,<sup>4</sup> A. Jungclaus,<sup>9</sup> K. Keyes,<sup>1</sup> V. Kumar,<sup>1</sup> S. Lunardi,<sup>8</sup> N. Mărginean,<sup>5,10</sup> G. Montagnoli,<sup>8</sup> D. R. Napoli,<sup>5</sup> F. Nowacki,<sup>3</sup> J. Ollier,<sup>1,11</sup> D. O'Donnell,<sup>1,12</sup> A. Papenberg,<sup>1</sup> G. Pollarolo,<sup>13</sup> M.-D. Salsac,<sup>14</sup> F. Scarlassara,<sup>8</sup> J. F. Smith,<sup>1</sup> K. M. Spohr,<sup>1</sup> M. Stanoiu,<sup>10</sup> A. M. Stefanini,<sup>5</sup> S. Szilner,<sup>5,15</sup> M. Trotta,<sup>5</sup> and D. Verney<sup>4</sup>

<sup>1</sup>*School of Engineering and Computing, University of the West of Scotland, Paisley PA1 2BE, United Kingdom, and The Scottish Universities Physics Alliance (SUPA)*

<sup>2</sup>*Laboratoire de Physique Appliquée et Théorique, Université Larbi Tébessa, Tébessa, Algérie*

<sup>3</sup>*IPHC, UMR7178, CNRS-IN2P3, and Université de Strasbourg, F-67037 Strasbourg Cedex 2, France*

<sup>4</sup>*IPN, IN2P3-CNRS and Université Paris-Sud, F-91406 Orsay Cedex, France*

<sup>5</sup>*INFN, Laboratori Nazionali di Legnaro, I-35020 Legnaro, Padova, Italy*

<sup>6</sup>*Schuster Laboratory, University of Manchester, Manchester M13 9PL, United Kingdom*

<sup>7</sup>*MTA ATOMKI, P.O. Box 51, H-4001 Debrecen, Hungary*

<sup>8</sup>*Dipartimento di Fisica and INFN-Sezione di Padova, Università di Padova, I35131 Padova, Italy*

<sup>9</sup>*Instituto de Estructura de la Materia, CSIC, E-28006 Madrid, Spain*

<sup>10</sup>*Horia Hulubei National Institute of Physics and Nuclear Engineering-IFIN-HH, Strasse Atomistilor No. 407, P.O. BOX MG-6, Bucharest-Magurele, Romania*

<sup>11</sup>*STFC Daresbury Laboratory, Warrington WA4 4AD, United Kingdom*

<sup>12</sup>*Oliver Lodge Laboratory, University of Liverpool, Liverpool L69 7ZE, United Kingdom*

<sup>13</sup>*Dipartimento di Fisica Teorica, Università di Torino, and INFN-Sezione di Torino, Via Pietro Giuria 1, I-10125 Torino, Italy*

<sup>14</sup>*CEA-Saclay, Service de Physique Nucléaire, 91191 Gif-sur-Yvette, France*

<sup>15</sup>*Ruder Bošković Institute, Zagreb, Croatia*

(Received 9 April 2015; published 9 October 2015)

The neutron-rich nuclei  $^{34,35,36,37,38}\text{P}$  were populated in binary grazing reactions initiated by a beam of  $^{36}\text{S}$  ions at 215 MeV incident on a thin  $^{208}\text{Pb}$  target. The combination of the PRISMA magnetic spectrometer and the CLARA array of escape-suppressed Ge detectors was used to detect  $\gamma$  rays in coincidence with projectile-like nuclear species. Further evidence to support the observed  $\gamma$  decay of excited states of the populated phosphorus isotopes is provided by  $\gamma$ - $\gamma$  coincidence measurements based on the results of an earlier thick-target deep-inelastic experiment. Level schemes for  $^{34,35,36,37,38}\text{P}$  are presented and discussed within the context of state-of-the-art shell-model calculations. In particular, new spin and parity assignments are proposed for a number of excited states of  $^{36}\text{P}$ . The evolution with neutron number of the energy difference of the low-lying  $J^\pi = 3/2^+$  and  $1/2^+$  states in the odd- $A$  isotopes of phosphorus, as well as the relationship to nuclear collectivity, is discussed. The evolution with neutron number of the shell-model wave functions of the first  $J^\pi = 1/2^+$ ,  $3/2^+$ , and  $5/2^+$  states of the odd- $A$  phosphorus isotopes and of the first  $J^\pi = 3^+$ ,  $4^-$ , and  $5^-$  states of the even- $A$  isotopes is also explored.

DOI: [10.1103/PhysRevC.92.044308](https://doi.org/10.1103/PhysRevC.92.044308)

PACS number(s): 23.20.Lv, 25.70.Lm, 27.30.+t

## I. INTRODUCTION

Neutron-rich phosphorus isotopes, with  $N = 20$  to 28, are ideal candidates for studying the evolution of single-particle states as the  $f_{7/2}$  neutron shell is being filled. For example, it has been shown experimentally that, in the odd-mass potassium ( $Z = 19$ ), chlorine ( $Z = 17$ ), and phosphorus ( $Z = 15$ ) isotopic chains, there is a reduction in the difference in excitation energy of the  $J^\pi = 3/2_1^+$  and  $1/2_1^+$  (ground) states with increasing neutron number for  $N = 20$ –28 [1]. The increase in binding of the  $1d_{3/2}$  proton with respect to the  $2s_{1/2}$  proton with increasing occupation of the  $1f_{7/2}$  neutron shell has been attributed to the monopole component of the tensor interaction, which results in an attractive force between neutrons in the  $j_> f_{7/2}$  orbital and protons in the

$j_< 1d_{3/2}$  orbital [2]. The energy difference of the  $1/2_1^+$  and  $3/2_1^+$  states is well reproduced in the isotopes of K, Cl, and P in  $0\hbar\omega$  shell-model calculations which use the latest SDPF-U interaction [3]. In  $N = 20$   $^{35}\text{P}$ , the binding energy gap,  $E(1/2_1^+) - E(3/2_1^+)$ , is approximately 2.5 MeV [4], while in  $^{37}\text{P}$  it has decreased to 0.86 MeV [5]. For the isotopes of potassium, where the energy spacing has been measured using proton pickup reactions [6,7], the total monopole shift between  $1d_{3/2}$  and  $2s_{1/2}$  proton binding is about 350 keV per  $1f_{7/2}$  neutron [8]. Eventually, with increasing neutron number, there is an inversion of the  $J^\pi = 3/2^+$  and  $1/2^+$  states, and this was first observed in the potassium isotopes [9] as long ago as 1967. The reasons for the inversion were not understood at that time. Inversion of the  $J^\pi = 3/2_1^+$  and  $1/2_1^+$  states was first observed in the isotopes of Cl by Liang *et al.* [10]. No such inversion has so far been reported in the phosphorus isotopes for  $N \leq 28$  [1,11].

\*Robert.Chapman@uws.ac.uk

The role of intruder states in the structure of nuclei within the so-called “island of inversion” near neutron number 20 has been the subject of much experimental work since the observation of increased binding energies of the ground states of  $^{31,32}\text{Na}$  [12]. More direct experimental evidence of strong deformation in this tightly circumscribed region of the nuclear landscape was based on the low excitation energy of the first  $2^+$  state [13,14] and the large  $B(E2; 0_1^+ \rightarrow 2_1^+)$  value [15–17] for  $^{32}\text{Mg}$ . Within a shell-model context, these effects have been described in terms of two-particle two-hole intruder configurations [18,19], intrinsically deformed. The tensor nucleon-nucleon force between protons in the  $j_{>} 1d_{5/2}$  orbital and neutrons in the  $j_{<} 1d_{3/2}$  orbital is believed to play a role in the reduction of the  $N = 20$  shell gap [2]. Nevertheless, the presence of such intruder states at low excitations in neutron-rich nuclei continues to challenge theoretical understanding. It is thus important to study the structure of nuclei and, in particular, of intruder states, not only within the island of inversion, but also for those nuclei which lie on the periphery of this region.

Another common feature in the odd-mass phosphorus nuclei, which is supported by comparisons with the results of shell-model calculations, is the observation that higher-lying states, above the first excited state, may be described in terms of a single proton coupled to excitations of the core. Thus, the good agreement found with the results of shell-model calculations suggests that the excited states of  $^{37}\text{P}$ , observed in binary grazing reactions [5], may be described in terms of the coupling of a  $2s_{1/2}$  or  $1d_{3/2}$  proton to the  $J^\pi = 2^+, 4^+, 6^+$  states of  $^{36}\text{Si}$  [20]. More recently, Bastin *et al.* [21] proposed that a  $2s_{1/2}$  or  $1d_{3/2}$  proton coupled to the  $2_1^+$  states in  $^{40,42}\text{Si}$  may explain the observed excited states at about 1 MeV in  $^{41,43}\text{P}$ , respectively. We are unable to access such neutron-rich phosphorus isotopes in the present work. In general, however, the study of the odd-mass phosphorus isotopes with  $20 \leq N \leq 28$  has, to date, been limited to the population of relatively low spin states, and in some cases only a few excited states are known. In the present work, we attempt to address this deficiency.

The present work forms one of several studies of neutron-rich nuclei in the *sdpf* shell, which are based on results from the same experiment. To date, we have reported on the structure of  $^{36}\text{Si}$  [20],  $^{37}\text{P}$  [5],  $^{40}\text{S}$  [22],  $^{38}\text{Cl}$  [23],  $^{33}\text{Si}$  [24], and  $^{41}\text{S}$  [25]. Earlier related studies of neutron-rich nuclei populated in deep-inelastic collisions with thick targets have focused on the structure of  $^{34}\text{P}$  [26],  $^{36}\text{S}$  [27], and  $^{41}\text{Cl}$  [10,28]. These published works are mainly concerned with the role of negative-parity intruder orbitals in the structure of neutron-rich nuclei on the periphery of the island of inversion.

In this paper, we present results on the odd-odd nuclei,  $^{34,36,38}\text{P}$ , and on the odd- $A$  nuclei,  $^{35,37}\text{P}$ . The yrast states of  $^{37}\text{P}$  were discussed in an earlier publication [5] and are revisited here to compare the level structure with the results of a more recent shell-model calculation. The  $(0 + 1) \hbar\omega$  states in the phosphorus isotopes with  $A = 34, 35$ , and  $36$  are described with the PSDPF interaction and the  $0 \hbar\omega$  states in the isotopes with  $A = 37$  and  $38$  are studied with the SDPF-U interaction. Details of these interactions are given later. The shell-model calculations were performed using the NATHAN code [29,30].

## II. EXPERIMENTAL METHOD

Excited states of neutron-rich Si, P, S, Cl, and Ar species, including the isotopes of P with  $A = 32\text{--}38$ , were populated in binary grazing reactions using a beam of  $^{36}\text{S}$  ions at 215 MeV delivered onto a thin  $^{208}\text{Pb}$  target using the combination of XTU tandem Van de Graaff accelerator and ALPI superconducting linear accelerator at the INFN Legnaro National Laboratory, Italy. The stable isotope of P is  $N = 16$   $^{31}\text{P}$ ; in the present work we have studied the spectroscopy of the P isotopes up to seven neutrons from stability. The experiment, which ran for a period of 6 days, involved the use of a beam of  $^{36}\text{S}^{9+}$  ions of average current 7 pA. The  $^{208}\text{Pb}$  target had a thickness of  $300 \mu\text{g cm}^{-2}$ , was isotopically enriched to 99.7%, and had a carbon backing of thickness  $20 \mu\text{g cm}^{-2}$ . The PRISMA magnetic spectrometer was used in conjunction with the CLARA Ge multidetector array to detect and identify the projectile-like species produced in multinucleon binary grazing reactions, in coincidence with their associated  $\gamma$  rays. Ion position information, measured at the entrance and exit to the magnetic elements, allowed the path of each ion through the PRISMA spectrometer to be reconstructed. This, together with time-of-flight measurements, enabled the velocity vector of the projectile-like species at the  $^{208}\text{Pb}$  target to be determined for each ion which passed through the spectrometer, thus allowing the Doppler correction of  $\gamma$ -ray energies to be performed on an event-by-event basis.

PRISMA is a large acceptance magnetic spectrometer and consists of a quadrupole singlet followed by a dipole magnet [31]. A microchannel plate [32], positioned at the entrance to the spectrometer, is used to obtain the  $x$  and  $y$  coordinates and time information of each ion that enters the spectrometer. A focal plane detector system at the exit to the spectrometer consists of a multiwire parallel-plate avalanche chamber (MWPPAC), followed downstream by an ionization chamber. The MWPPAC [33] provides  $x$ ,  $y$ , and time information of each ion after it has passed through the magnetic dipole, while the ionization chamber, divided into  $10 \times 4$  sections, measures  $\Delta E$  and  $E$  [33]. Measurements taken with the PRISMA magnetic spectrometer enable a determination of the atomic number  $Z$ , the mass number  $A$ , the ionic charge state, and the absolute velocity vector of each ion that reaches the detector system at the focal plane. PRISMA has a solid angle of 80 msr, a momentum acceptance of  $\pm 10\%$ , and a mass resolution of  $1/300$  via time-of-flight measurements. In this experiment, PRISMA was set at angle of  $56^\circ$  with respect to the incident  $^{36}\text{S}$  beam direction, and this is near to the laboratory grazing angle of  $58^\circ$ .

CLARA [34] is a high-granularity  $\gamma$ -ray array, consisting of 25 EUROBALL escape-suppressed hyperpure Ge clover detectors mounted in a hemispherical shaped frame; 22 detectors were available during the experiment. The CLARA array has a photopeak efficiency of about 3%, has a peak-to-total ratio of 0.45 for  $^{60}\text{Co}$  1332-keV  $\gamma$  rays, and covers an azimuthal angular range of  $\theta = 104^\circ$  to  $180^\circ$  with respect to the entrance aperture of the PRISMA magnetic spectrometer. Following Doppler-shift energy correction of  $\gamma$  rays from projectile-like species, the full width at half maximum (FWHM) of  $\gamma$ -ray photopeaks is approximately 0.7% in energy. A relative

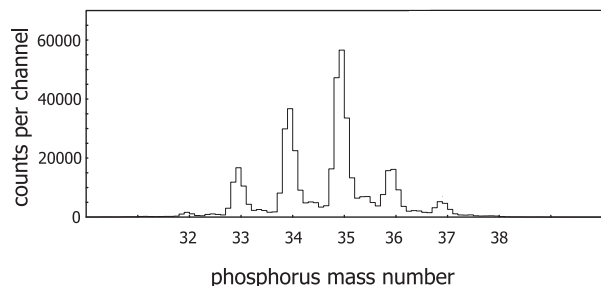


FIG. 1. A mass spectrum showing the isotopes of phosphorus populated in the present work.

photopeak efficiency calibration for the CLARA array was carried out using radioactive sources of  $^{152}\text{Eu}$ ,  $^{133}\text{Ba}$ , and  $^{56}\text{Co}$ . The measurement of  $\gamma$  rays in time coincidence with projectile-like species detected and identified at the focal plane of PRISMA leads to an unambiguous association of  $\gamma$ -ray transitions with a nucleus of specific  $Z$  and  $A$ .

### III. RESULTS AND DISCUSSION

The mass spectrum of Fig. 1 shows that the phosphorus isotopes with mass numbers  $32 \leq A \leq 38$ , i.e., up to seven neutrons from stability, were successfully populated in the present work.  $^{38}\text{P}$  was weakly populated and the corresponding mass peak is not clearly visible in the spectrum presented here. The measured mass resolution is  $1/140$ . A mass gate of suitable location and width is used to produce a one-dimensional  $\gamma$ -ray spectrum corresponding to the particular isotope of interest.

The odd-odd nuclei,  $^{34,36,38}\text{P}$ , and the odd- $A$  nuclei,  $^{35,37}\text{P}$ , are discussed here. As noted earlier, the yrast states of  $^{37}\text{P}$  were discussed in an earlier publication [5]. Level schemes were constructed in the present work from a consideration of  $\gamma$ -ray energy-sum relationships,  $\gamma$ -ray relative intensities, the population characteristics of multinucleon transfer reactions, and results from published experimental work. The multiplicities of  $\gamma$ -ray transitions were not determined; consequently, the spins and parities of the states populated in the present work could not be explicitly established. The spin and parity assignments in the level schemes presented here come from published work and are included for completeness. Where new spin and parity assignments are tentatively proposed here, these are based on three considerations, namely the observation that multinucleon transfer reactions preferentially populate yrast and near-yrast states [10,35–38], on the observed  $\gamma$ -ray feeding and decay of the state, and, finally, on comparisons with the results of shell-model calculations, also presented here. Unfortunately, the relatively low statistics of the present experiment preclude the measurement of  $\gamma$ -ray coincidences.

To confirm earlier assignments and to strengthen the evidence for the placement of previously unobserved  $\gamma$ -ray transitions within the phosphorus level schemes, triples  $\gamma$ -ray data from an earlier deep-inelastic experiment [39], which studied the nuclear structure of projectile- and target-like species resulting from the interaction of 230 MeV  $^{36}\text{S}$  ions with a thick target of  $^{176}\text{Yb}$ , were revisited.

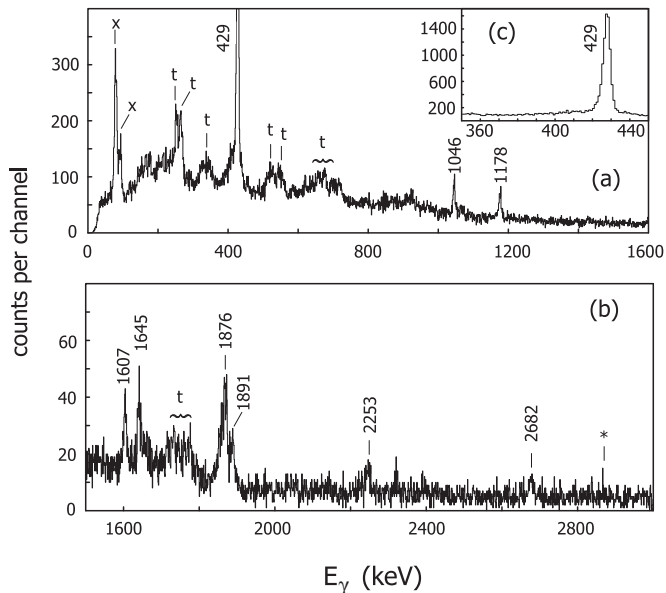


FIG. 2. Sections of an energy spectrum of  $\gamma$  rays measured in time coincidence with  $Z = 15$ ,  $A = 34$  reaction products detected at the PRISMA focal plane. Panels (a) and (b) correspond to  $\gamma$ -ray energies up to 1600 keV and from 1500 to 3000 keV, respectively, and panel (c) shows the 429-keV photopeak.

#### A. $^{34}\text{P}$

Figure 2 shows sections of an energy spectrum of  $\gamma$  rays observed in coincidence with  $Z = 15$ ,  $A = 34$  reaction products, detected and identified at the PRISMA focal plane. In this, and in all subsequent figures of  $\gamma$ -ray spectra, the peaks labeled “x” are Pb x rays, while those labeled “t” are incorrectly Doppler-corrected  $\gamma$  rays associated with the unobserved slower-moving complementary target-like fragments, namely the isotopes of  $^{83}\text{Bi}$ . The energies of  $\gamma$  rays associated with the deexcitation of  $^{34}\text{P}$  excited states have uncertainties of about  $\pm 1$  keV and are listed, together with their associated measured relative intensities, in Table I.

The publication of Ollier *et al.* [26] summarized the experimental situation in relation to the study of the states of  $^{34}\text{P}$  prior to the more recent works of Bender *et al.* [40,41] and of Chakrabarti *et al.* [42]. The lifetime of the  $J^\pi = 4^-$  intruder state at an excitation energy of 2305 keV has also recently been measured by Mason *et al.* [43]. These recent investigations employed the  $^{18}\text{O} (^{18}\text{O}, pn)$  fusion-evaporation reaction to study the nuclear structure of  $^{34}\text{P}$ . In the present work, seven previously observed [26,37,40–42,44,45]  $\gamma$ -ray transitions at energies of 429, 1046, 1178, 1607, 1645, 1876, and 1891 keV and two previously unreported transitions at energies of 2253 and 2682 keV have been identified. In the most recent work by Bender *et al.* [41], many hitherto unobserved transitions were identified. Neutron-rich  $^{34}\text{P}$ , while three neutrons from the stable  $^{31}\text{P}$  isotope, is accessible to study by fusion evaporation reactions which have, in general, larger cross sections than multinucleon transfer reactions; consequently, detailed spectroscopy is possible when large arrays of escape-suppressed germanium detectors are employed to detect the

TABLE I. The measured relative intensities of  $^{34}\text{P}$ ,  $^{35}\text{P}$ , and  $^{36}\text{P}$   $\gamma$ -ray photopeaks presented in order of increasing  $\gamma$ -ray energy.

$^{34}\text{P}$		$^{35}\text{P}$		$^{36}\text{P}$	
$E_\gamma$ (keV)	$I_\gamma$ (relative units)	$E_\gamma$ (keV)	$I_\gamma$ (relative units)	$E_\gamma$ (keV)	$I_\gamma$ (relative units)
429	100.0(13)	127	5.2(6)	152	2.73(61)
1046	9.60(66)	241	32.6(9)	174	18.8(9)
1178	10.23(74)	273	12.9(8)	249	100.0(38)
1607	6.12(65)	323	12.9(8)	423	8.41(91)
1645	6.96(66)	392	24.9(11)	471	5.86(92)
1876 <sup>a</sup>	24.4(11)	469	16.8(11)	614	12.1(13)
1891	7.13(60)	633	10.4(9)	921	13.4(14)
2253	5.76(61)	665	17.8(10)	2030	36.2(20)
2682	4.63(57)	861	9.8(12)	3182	18.6(17)
		1353	9.2(11)		
		1474	16.4(14)		
		1592	7.7(10)		
		1994	14.2(12)		
		2386	99.2(28)		
		3860	100.0(32)		

<sup>a</sup>See discussion in text in relation to the measured photopeak centroid.

$\gamma$  rays from the decay of populated excited states. Under these conditions, measurements of  $\gamma$ -ray coincidences,  $\gamma$ -ray

angular distributions, and  $\gamma$ -ray linear polarization, essential for the unambiguous construction of decay schemes and assignments of  $J^\pi$  values, are possible. The transitions at energies of 2403 keV (tentative) and 2885 keV, first observed in the thick-target deep-inelastic experiment of Ollier *et al.* [26], were not seen in the present work, but have been observed by Bender *et al.* [40,41]; the 2885-keV transition, but not that at 2403 keV, was observed in the work of Chakrabarti *et al.* [42]. The  $\gamma$ -ray angular distribution measurements of Bender *et al.* [40] are consistent with the  $J^\pi$  values of  $3^-$ ,  $5^-$ , and  $7^+$  proposed by Ollier *et al.* for the excited states at 2320, 3351, and 6236 keV, respectively.

Figure 3 shows the  $^{34}\text{P}$  level scheme based on the present work together with level schemes from earlier works [26,41,44–46]. The level scheme proposed here is consistent with the work of Ollier *et al.* [26], which is based on the population of projectile-like species in deep-inelastic reactions induced by 230-MeV  $^{36}\text{S}$  ions incident on a thick target of  $^{176}\text{Yb}$  and with the more recent work of Bender *et al.* [41], which, as noted earlier, involved the fusion-evaporation reaction  $^{18}\text{O} (^{18}\text{O}, pn)$ . The 1645-keV transition, which was observed in the work of Bender *et al.* [40,41] and assigned to a  $J^\pi = 5^-$  to  $4^-$  transition, but was not reported by Ollier *et al.*, has also been identified in the present work. In support of this assignment, Fig. 4 shows double-gated  $\gamma$ -ray spectra from a  $\gamma\gamma\gamma$  data cube, referred to above. Figure 4(c)

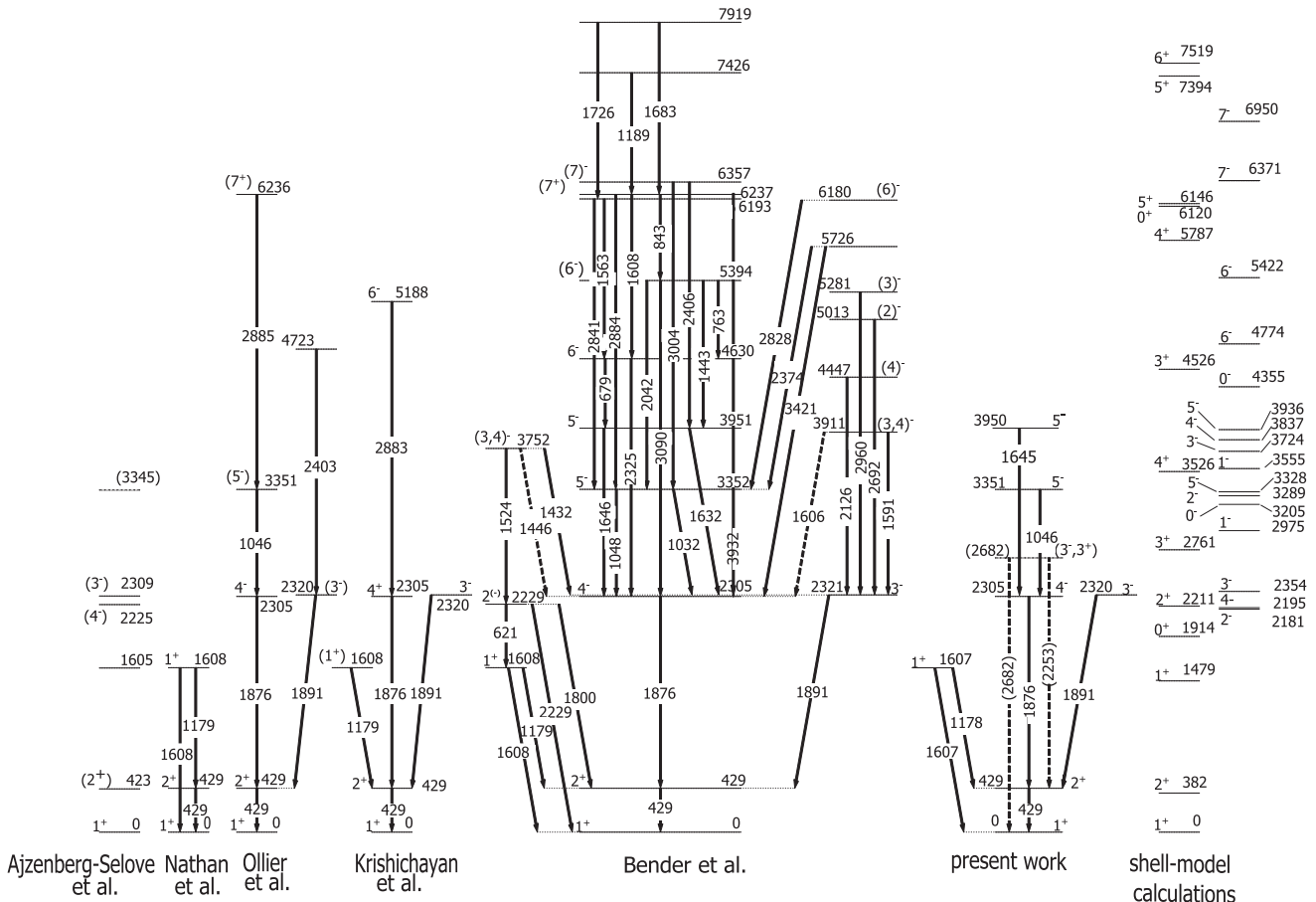


FIG. 3. Experimental level schemes of  $^{34}\text{P}$  from Refs. [26,41,44–46] and from the present work. Also shown are results from the shell model using the  $1\hbar\omega$  PSDPF interaction. See text for details.

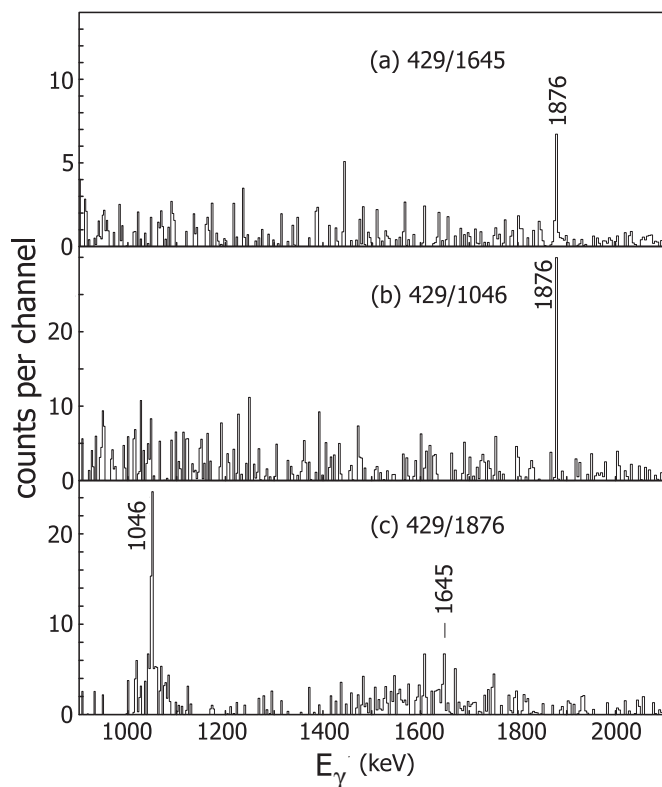


FIG. 4. Double-gated  $\gamma$ - $\gamma$  coincidence spectra from an earlier deep-inelastic experiment, corresponding to transitions in  $^{34}\text{P}$ . See text for details of the gating conditions.

shows the  $\gamma$ -ray spectrum corresponding to a double  $\gamma$ -ray coincidence gate placed on the 429- and 1876-keV transitions; there is clearly a strong photopeak at 1046 keV, as earlier reported by Ollier *et al.*, but there is also a much weaker photopeak at 1645 keV, indicating that both the 1046- and the 1645-keV  $\gamma$  rays are in coincidence with the  $\gamma$ -ray transitions at 429 and 1876 keV. The double-gated  $\gamma$ -ray coincidence spectra in Figs. 4(a) and 4(b), corresponding to the first gate set on the 429-keV  $\gamma$  ray and the second on the 1645- and 1046-keV  $\gamma$ -ray peaks, respectively, show that, while the 1645- and 1046-keV  $\gamma$  rays are in coincidence with the 429- and 1876-keV transitions, they are not in coincidence with each other. The 1645-keV  $\gamma$ -ray transition has therefore been assigned to the depopulation of an excited state in  $^{34}\text{P}$  at 3950 keV, in agreement with the published level schemes of Bender *et al.* [40,41]. The present results are also consistent with the earlier observation of the depopulation of the  $^{34}\text{P}$  1607-keV excited state by the emission of 1178- and 1607-keV  $\gamma$  rays, first observed by Nathan *et al.* [44] in a  $^{34}\text{Si}$   $\beta$ -decay study. The measured relative intensities of  $\gamma$  rays depopulating the 1607-keV excited state are also in good agreement with the  $\beta$ -decay measurements of Nathan *et al.* and with the results of Bender *et al.* [40,41]. In the latter work, two unresolved transitions of energy 1608 keV were identified. The second, previously unobserved, member of the doublet was assigned to the decay of the 6237-keV  $J^\pi = (7^+)$  state to the 4630-keV  $J^\pi = 6^-$  state. The observation that the branching ratio of the 1607-keV excited state measured in the present work is

consistent, within experimental errors, with the value quoted by Bender *et al.* would strongly indicate that the  $(7^+)$  state at 6237 keV does not receive any significant population in the present work; in addition, none of the associated decay  $\gamma$  rays is observed in the spectrum of Fig. 2. In the published  $\gamma$ -ray spectrum of Ollier *et al.* [26], there are two unlabeled  $\gamma$ -ray photopeaks at energies of 1606 and 1645 keV which are in coincidence with the double gate on the 429- and 1876-keV transitions; this is consistent with the level scheme of Bender *et al.* [40,41] and, in particular, with their observation of an unresolved doublet at 1608 keV.

The two previously unreported  $\gamma$  rays at energies of 2253 and 2682 keV differ in energy by 429 keV; consequently, it is very tentatively proposed here that the transitions correspond to the decay of a previously unknown  $^{34}\text{P}$  state at 2682 keV to the first excited state at 429 keV and to the ground state, respectively. The very tentative  $J^\pi$  value of  $(3^+, 3^-)$  is based on the assumption that the decays are dipole or quadrupole in nature and that the populated state is yrast or near yrast.

From a  $\gamma$ -ray coincidence analysis of data collected in a deep-inelastic study, which involved the interaction of a beam of  $^{37}\text{Cl}$  ions at 167 MeV with a target of  $^{160}\text{Gd}$ , Fornal *et al.* [37] identified an 1876-keV  $\gamma$  ray associated with the deexcitation of an excited state of  $^{34}\text{P}$  at 2305 keV. This observation was later confirmed by Ollier *et al.* [26], by Krishichayan *et al.* [45], and by Bender *et al.* [40]. The  $\gamma$ -ray photopeak labeled at 1876 keV (see Fig. 2) has an unusually large width which may be accounted for by the lifetime of the decaying state. Asai *et al.* [47] determined the half-life of the 2305-keV excited state to be  $0.3 < t_{1/2} < 2.5$  ns. More recently, the half-life has been measured by Mason *et al.* [43] as  $2.0 \pm 0.1$  ns. In the present work, Doppler correction is undertaken with the assumption that  $\gamma$  rays are emitted from the target position. However, for a nanosecond isomeric state in a nucleus moving with approximately 10% of the velocity of light, this assumption is no longer a good approximation and, in this case, the applied Doppler correction leads to a broadening in energy of the photopeak and a shift in the peak centroid. On this basis, the broad photopeak at about 1876 keV is assumed to correspond to the isomeric 1876-keV  $\gamma$ -ray transition.

As noted earlier, the 2885-keV  $\gamma$  ray, which depopulates the  $J^\pi = (7^+)$  state [26] was not observed in the present work; its expected location in the  $^{34}\text{P}$   $\gamma$ -ray spectrum of Fig. 2 is indicated by the label “\*”. The relative intensities of the 1046- and 2885-keV  $\gamma$  rays measured by Ollier *et al.* [26] would suggest that the intensity of the 2885-keV  $\gamma$  ray in the present work is much smaller than those of the weak photopeaks at 2253 and 2682 keV.

In the context of the simple shell model, the ground state of  $^{34}\text{P}$  is expected to have a  $J^\pi$  value of  $1^+$  or  $2^+$ , resulting from the unpaired  $2s_{1/2}$  proton coupled to a  $1d_{3/2}$  neutron hole. The results of shell-model calculations carried out using the  $1 \hbar\omega$  PSDPF interaction [48] show that these configurations represent 71% and 75% of the wave functions of the  $1^+$  and  $2^+$  states, respectively. This shell-model calculation has a  $^4\text{He}$  core and uses the full  $p$ - $sd$ - $pf$  model space; it is built on existing interactions for the major shells with adjustments of the cross-shell parameters. The positive-parity states are

essentially obtained using the USDB Hamiltonian, developed by Brown and Richter [49], which is included in the  $p$ - $sd$ - $pf$  interaction. Excitation of one nucleon is allowed across a major shell, from the  $sd$  shell to the  $pf$  shell in the present case.

The 2305-, 3351-, and 6236-keV excited states, identified by Ollier *et al.* [26], using triples  $\gamma$ -ray measurements, were tentatively assigned by these authors to have  $J^\pi$  values of  $4^-$ ,  $5^-$ , and  $7^+$  respectively, corresponding to the  $\pi(2s_{1/2})^1 \otimes \nu(1f_{7/2})^1$ ,  $\pi(1d_{3/2})^1 \otimes \nu(1f_{7/2})^1$ , and  $\pi(1f_{7/2})^1 \otimes \nu(1f_{7/2})^1$  stretched configurations. These proposed assignments, which, as noted earlier, are in agreement with the recent assignments of Bender *et al.* [40], were based on systematics and on the observation of a linear dependence of the  $np$  separation energies on mass number for the  $J^\pi = 4^-$ ,  $5^-$ , and  $7^+$  stretched states in the odd-odd P isotopes [26]. The previously observed  $J^\pi = 3^-$  state [46] is believed to be the other member of the doublet arising from the configuration  $\pi(2s_{1/2})^1 \otimes \nu(1f_{7/2})^1$ . In the PSDPF shell-model calculations performed here, the above suggested configurations of the  $J^\pi = 3^-$ ,  $4^-$ , and  $5^-$  states correspond to the largest components—33%, 36%, and 30%, respectively—of the wave functions. The experimental yrast  $J^\pi = 7^+$  state is not reproduced in the shell-model calculation, because it lies outside the model space. Within the restricted basis of the present shell-model calculations, the yrast  $7^+$   $sd$  state lies at a much higher excitation energy of 10.711 MeV and has as the dominant configuration (89% of the wave function)  $\pi(1d_{5/2})^{-2}(1d_{3/2})^1 \otimes \nu(1d_{3/2})^3$ . The wave functions of the  $J^\pi = 3^-$ ,  $4^-$ , and  $5^-$  states of the isotopic sequence for  $15 \leq N \leq 23$  are discussed later in the paper.

The results of  $1 \hbar\omega$  shell-model calculations based on the PSDPF interaction are presented in column 7 of Fig. 3. Only the first two states of a given  $J^\pi$  value are presented. There is excellent overall agreement with the published experimental level schemes; observed levels have a close-lying shell-model counterpart. The r.m.s. deviation between the published level scheme and the results of shell-model calculations is 70 keV. The first three states are positive-parity states of  $0p$ - $0h$  configuration; higher-lying positive-parity intruder states of  $2p$ - $2h$  configuration cannot be described within the context of the 0 and  $1 \hbar\omega$  PSDPF interaction. The proposed new state observed here at 2682 keV, with a suggested  $J^\pi$  value of  $(3^-, 3^+)$ , has a possible shell-model counterpart at an excitation energy of 2761 keV with a  $J^\pi$  value of  $3^+$ . The experimental level scheme suggests that the first 1-ph state of  $^{34}\text{P}$  lies at an excitation energy of 2305 keV and the first 2-ph state at 6236 keV.

## B. $^{35}\text{P}$

Figure 5 shows sections of a spectrum of  $\gamma$  rays detected in coincidence with the  $Z = 15$ ,  $A = 35$  reaction products identified at the focal plane of PRISMA.  $\gamma$ -ray transitions observed in the present work have an uncertainty in energy of about  $\pm 1$  keV and are listed in Table I together with measured relative intensities.

Previous investigations of the level structure of  $^{35}\text{P}$  include a study of the  $(d, ^3\text{He})$  reaction, first by Thorn *et al.* [50] and later by Khan *et al.* [4]. In the  $(d, ^3\text{He})$  experiment of Khan *et al.*, 52-MeV vector polarized deuterons were used

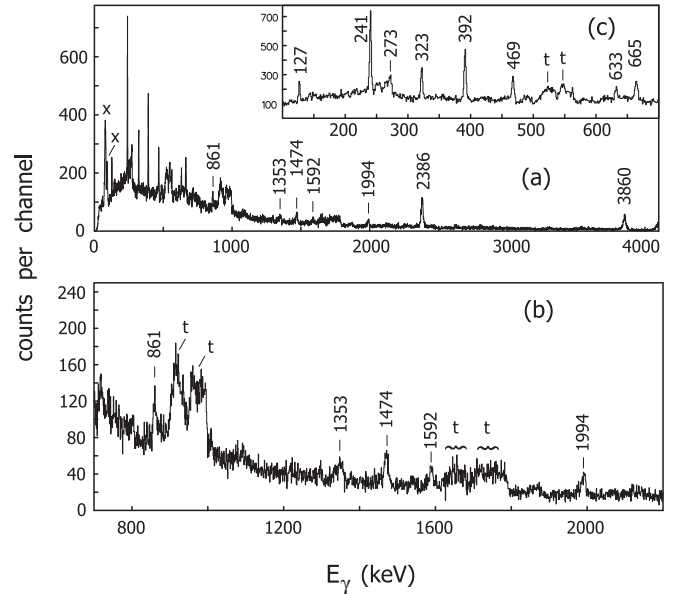


FIG. 5. Sections of the spectrum of  $\gamma$  rays detected in coincidence with  $Z = 15$ ,  $A = 35$  reaction products detected at the PRISMA focal plane. Panel (a) corresponds to the full  $\gamma$ -ray energy range, while the lower spectrum (b) shows more clearly the  $\gamma$ -ray photopeaks between 750 keV and 2.2 MeV. Panel (c) shows the low-energy spectrum, from 100 to 700 keV, in more detail.

in a determination of the  $l$  values and spectroscopic factors for direct proton pickup from the  $^{36}\text{S}$  ground state to states of  $^{35}\text{P}$ . To establish the  $j$  value ( $j_>$  or  $j_<$ ) of the transferred proton, polarization measurements were also performed. The authors [4] reported that the excited states, previously observed by Thorn *et al.* [50], all have  $J^\pi$  values of  $5/2^+$ , indicating that the  $\pi(2s_{1/2})^2(1d_{5/2})^{-1}$  proton two-particle-one-hole strength is fragmented in  $^{35}\text{P}$ . Experimentally, the summed spectroscopic strength for proton  $d_{5/2}$  pickup from the ground state of  $^{36}\text{S}$  is  $\Sigma C^2S = 5.35$ , which is close to the sum-rule limit of 6. More than half of the strength (2.9) is located in the first  $5/2^+$  state at 3857 keV. A  $J^\pi = 3/2^+$  state at 2386 keV was also identified by Khan *et al.*, in addition to two further states at 4474 and 7520 keV, for which no  $J^\pi$  assignments were made. The observation of  $d_{3/2}$  proton pickup strength indicates that there is a  $2p$ - $2h$  component,  $\pi(1d_{3/2})^2(2s_{1/2})^{-2}$ , in the  $^{36}\text{S}$  ground-state wave function, corresponding to approximately 8% of full occupancy of the proton  $1d_{3/2}$  shell-model state. Within the uncertainties associated with a distorted-wave Born approximation analysis of single-nucleon transfer, this is not inconsistent with an occupation of the  $2s_{1/2}$  proton shell-model state in the  $^{36}\text{S}$  ground state of about 80%, a value based on the proton pickup strength measured by Khan *et al.* [4].

Following the work of Khan *et al.*, Dufour *et al.* [51] reported the measured  $\gamma$ -ray energies and intensities of transitions in  $^{35}\text{P}$ , following the  $\beta$  decay of  $^{35}\text{Si}$ . The transitions were later presented in a proposed level scheme by Orr *et al.* [52]; see Fig. 6.

The recent work of Wiedeking *et al.* [53] is currently the most comprehensive published spectroscopic  $\gamma$ -ray study of  $^{35}\text{P}$ . These authors used the one-proton transfer reaction,

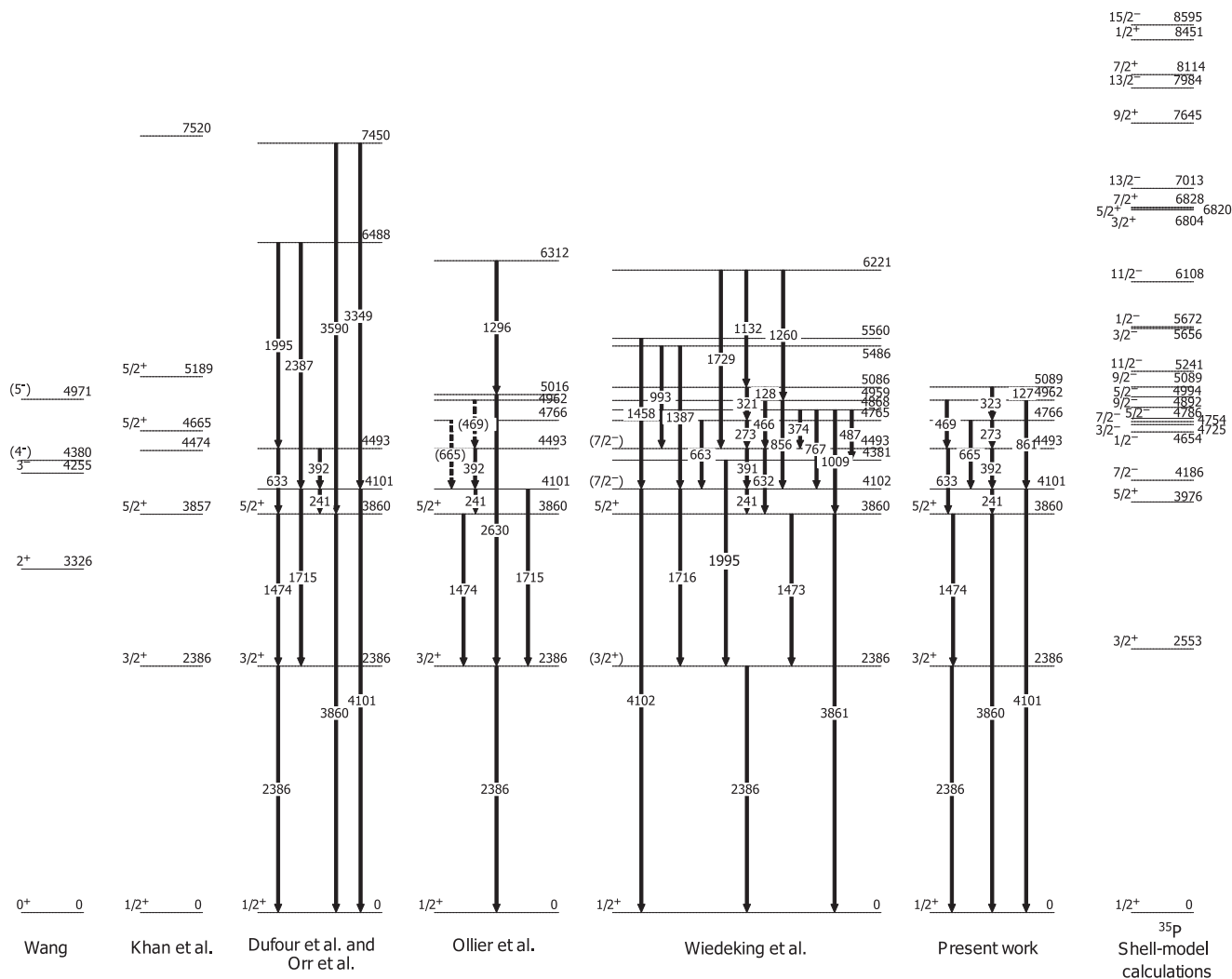


FIG. 6. The  $^{35}\text{P}$  level scheme constructed from the present work together with those produced from previous work [4,39,51–53]. The results of a  $1\hbar\omega$  shell-model calculation based on the PSDPF interaction are also presented. A level scheme of  $^{34}\text{Si}$  is also included in the first column [54]. See text for details.

$^{208}\text{Pb}$  ( $^{36}\text{S}$ ,  $^{35}\text{P}$ ), at a beam energy of 230 MeV, to populate the final nucleus. Binary reaction products were detected in coincidence in CHICO, a heavy-ion parallel-plate avalanche counter array, and coincident  $\gamma$  rays were detected using the Gammasphere array of escape-suppressed Ge detectors. A second experiment, with the same nucleon-transfer process, made use of a thick target of  $^{208}\text{Pb}$ , and  $\gamma$  rays were also detected using Gammasphere.

The  $^{35}\text{P}$  level scheme of the present work is shown in Fig. 6. It was constructed by identifying possible  $\gamma$ -ray energy-sum relationships, from a consideration of measured relative transition intensities, and from a reanalysis of  $\gamma\gamma\gamma$  triples coincidence data from an earlier thick-target experiment [39], which studied the nuclear structure of projectile- and target-like species resulting from the interaction of 230-MeV  $^{36}\text{S}$  ions with  $^{176}\text{Yb}$ . Previous experimental work [4,39,52,53] was also used as a guide. Typical examples of double-gated  $\gamma$ -ray spectra obtained from the  $\gamma\gamma\gamma$  data cube are shown in Fig. 7. Figure 7(a) shows a  $\gamma$ -ray spectrum which results from a

double gate placed on the 127- and 469-keV transitions;  $\gamma$ -ray photopeaks of energy 241, 392, and 633 keV are observed, as expected. In addition, there are no  $\gamma$ -ray photopeaks at energies of 273, 323, and 665 keV, in accordance with the level scheme of Fig. 6. Figure 7(b) shows a  $\gamma$ -ray spectrum which results from a double gate placed on the 241- and 469-keV transitions;  $\gamma$ -ray photopeaks at 127 and 392 keV are clearly visible, indicating that both transitions are in coincidence with those at 241 and 469 keV and this is again consistent with the level scheme of Fig. 6. Additional confirmation is provided by the  $\gamma$ -ray spectra of Figs. 7(c) and 7(d), where the double gate placed on the 323- and 392-keV transitions indicates that the  $\gamma$  rays at energies of 241 and 273 keV are in coincidence with these two transitions, while the double gate placed on the 241- and 665-keV transitions shows a single photopeak at an energy of 323 keV.

$^{35}\text{P}$  level schemes from previous published studies are shown in Fig. 6 together with the  $^{35}\text{P}$  level scheme of the present work and the results of  $p$ - $sd$ - $pf$  shell-model

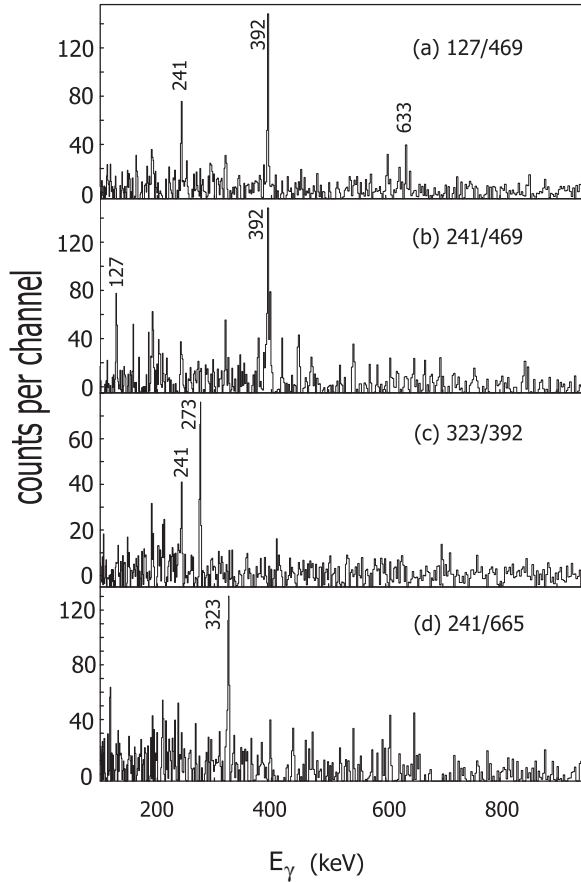


FIG. 7. Double-gated  $\gamma$ - $\gamma$  spectra from the  $\gamma\gamma\gamma$  data cube, which was constructed in an earlier deep-inelastic experiment. The spectra show the  $\gamma$ -ray coincidence relationships. See text for details.

calculations. It can be seen from Fig. 6 that the present level scheme is in agreement with the earlier level schemes and, in particular, with that of the most recent study by Wiedeking *et al.* [53]. With the exception of three  $\gamma$ -ray transitions at energies of 1353, 1592, and 1994 keV, which we have been unable to place within the level scheme, all of the  $\gamma$ -ray transitions observed here have previously been observed by Wiedeking *et al.* [53]. In addition, Wiedeking *et al.* observed a number of transitions, mainly decaying to states of excitation energy above about 4.1 MeV, and these transitions have not been observed in this or in other published works. In the work of Ollier *et al.* [39], transitions of energy 1296 and 2630 keV were observed and placed in the  $^{35}\text{P}$  level scheme (see Fig. 6); these transitions have not been observed in this or in other published work. In the present work, the nonobservation of the 1715-keV transition in the decay of the 4101-keV state may be explained by reference to Fig. 5(b), which shows the  $^{35}\text{P}$   $\gamma$ -ray spectrum for  $\gamma$  rays of energies from 750 to 2200 keV. The structure in Fig. 5 between 1.6 and 1.8 MeV is dominated by incorrectly Doppler-corrected  $\gamma$  rays associated with the slower moving complementary target-like fragment. Comparing the relative intensities of transitions observed both in the work of Dufour *et al.* [51] and those of the present work, it may be inferred that the broad structure

in Fig. 5 is obstructing the observation of the 1715-keV  $\gamma$ -ray photopeak.

As noted earlier, we have been unable to place the 1994-keV  $\gamma$  ray within the level scheme. The proposed placement of this transition by Orr *et al.* [52], corresponding to feeding the 4493-keV excited state, causes an intensity imbalance in the present work, suggesting that the 1994-keV  $\gamma$  ray in the  $^{35}\text{P}$  level scheme of Orr *et al.* is incorrectly placed, if it corresponds to a single transition. Based on intensity-balance arguments, the levels fed by the 1994-keV  $\gamma$ -ray transition are probably those at 2386 or 3860 keV. Wiedeking *et al.* [53] have assigned the 1994-keV transition to the decay of a state at 4381 keV to the 2386-keV state.

Figure 6 also shows the results of  $p$ - $sd$ - $pf$  shell-model calculations, which use the PSDPF interaction [48]. The first two levels of a given spin between  $1/2$  and  $15/2$  are included in the figure. The results of the shell-model calculations predict the first excited  $J^\pi = 3/2^+$  state at about 2.6 MeV, followed by a 1.5-MeV gap in excitation energy and a densely packed cluster of states spread over an energy of about 1 MeV, which is in overall good agreement with experiment. In terms of the single-particle shell model, the first  $J^\pi = 1/2^+$ ,  $3/2^+$ , and  $5/2^+$  states of  $^{35}\text{P}$  are expected to correspond to  $2s_{1/2}$  and  $1d_{3/2}$  proton states and a  $1d_{5/2}$  proton-hole state, respectively, with subsequent high-lying negative-parity states formed from the promotion of the unpaired proton across the  $Z = 20$  shell gap. At  $N = 20$ , the  $Z = 20$  shell gap is about 7 MeV, while the  $N = 20$  gap at  $Z = 14$  is about 5 MeV. The shell-model calculations indeed show that the  $J^\pi = 1/2^+$  ground state is a relatively pure (90%) proton  $2s_{1/2}$  state, while the 2386-keV  $J^\pi = 3/2^+$  state also has a relatively pure (91%)  $1d_{3/2}$  proton configuration. The  $J^\pi = 5/2^+$  state at 3860 keV corresponds, as expected, to the proton configuration  $(d_{5/2})^5 (s_{1/2})^2$  (89%). For these first two excited states, agreement between shell model and experiment, in relation to the reproduction of excitation energies, is good. Higher-lying positive-parity states are intruder states of  $2p$ - $2h$  configuration and cannot be described with the 0 and  $1\hbar\omega$  PSDPF interaction. Later in the paper, the structure of the first  $J^\pi = 1/2^+$ ,  $3/2^+$ , and  $5/2^+$  states are discussed for the odd- $A$  phosphorus isotopes with neutron numbers in the range  $20 \leq N \leq 28$ . The  $J^\pi = (7/2^-)$  state at an excitation energy of 4102 keV is the lowest lying intruder state of  $^{35}\text{P}$  observed experimentally. The shell-model counterpart is at an excitation energy of 4186 keV. For this state, the component of the wave function corresponding to a closed neutron shell and promotion of the odd proton from the  $2s_{1/2}$  to  $1f_{7/2}$  shell-model orbits corresponds to only about 20% of the wave function. The largest component (34%) corresponds to the configuration  $\pi(1d_{5/2})^6(2s_{1/2})^1 \otimes \nu(1d_{5/2})^6(2s_{1/2})^2(1d_{3/2})^3(1f_{7/2})^1$ , in which the neutron core is broken. The overall neutron occupancy of the  $1f_{7/2}$  shell is 0.58. The second  $J^\pi = 7/2^-$  state, at a predicted excitation energy of 4754 keV, is the first state with essentially single-neutron occupancy (0.95) of the  $1f_{7/2}$  shell. For the second  $J^\pi = 7/2^-$  state, there is a large component (65%) of the wave function corresponding to the  $J^\pi = 4^-$  neutron core coupled to protons with  $J^\pi = 1/2^+$ . The high-spin states predicted in the PSDPF shell-model calculation, with  $9/2^- \leq J^\pi \leq 19/2^-$  have wave functions corresponding, to a good approximation,



to single-neutron occupancy of the  $1f_{7/2}$  shell. In an earlier discussion of the phosphorus isotopes ( $A = 30$  to  $35$ ) with the results of shell-model calculations based on the PSDPF interaction, Bouhelal *et al.* [55] suggested that the states observed in  $^{35}\text{P}$  at 4766 and 4959 keV have a  $J^\pi$  value of  $9/2^-$ , while the states observed at 5086 and 6221 keV have a  $J^\pi$  value of  $11/2^-$ . These states, within the shell-model description, correspond to the coupling of an odd proton in the  $2s_{1/2}$  and  $1d_{3/2}$  shells to negative-parity states of the  $^{34}\text{Si}$  core. Thus, the major contribution to the configuration of the 5.241-MeV shell-model state with  $J^\pi = 11/2^-$  and that at 5.089 MeV with  $J^\pi = 9/2^-$  corresponds (72% and 66%, respectively) to the coupling of protons to spin  $1/2^+$  and neutrons to spin  $5^-$ . For the shell-model states at excitation energies of 6.108 MeV ( $J^\pi = 11/2^-$ ) and at 4.892 MeV ( $J^\pi = 9/2^-$ ) neutrons with spin  $4^-$  are coupled to protons with spin  $3/2^+$  and  $1/2^+$  (54% and 68%, respectively).

Following on from the above discussion of the  $9/2^-$  and  $11/2^-$  states, it is tempting to suggest that the dense cluster of states observed experimentally between approximately 4 and 6 MeV, predicted to be largely composed of negative-parity states, corresponds to the coupling of a single  $2s_{1/2}$  proton to excited states of the ( $^{34}\text{Si}$ ) neutron core. A single  $2s_{1/2}$  proton coupled to the  $J^\pi = 3^-$  of  $^{34}\text{Si}$  at 4255 keV [54], for example, would yield two states of  $^{35}\text{P}$  with  $J^\pi$  values of  $5/2^-$  and  $7/2^-$ . Figure 6 shows additional negative-parity states of  $^{34}\text{Si}$ , identified by Wang *et al.* [54], at 4380 and 4971 keV, which lie within the excitation energy range of the cluster of states observed in  $^{35}\text{P}$ . Coupling these negative-parity states of  $^{34}\text{Si}$  to a  $2s_{1/2}$  proton would yield states in  $^{35}\text{P}$  with  $J^\pi$  values between  $7/2^-$  and  $11/2^-$ . This coupling mechanism may represent a more energetically favorable alternative to the promotion of a nucleon across the  $Z = 20$  or  $N = 20$  shell gaps. The results of the PSDPF shell-model calculations do indeed show that such a coupling takes place, with a proton in the  $2s_{1/2}$  shell coupled to negative-parity states of the core accounting for approximately 40%–70% of the wave function. It has also been proposed earlier that excited states of  $^{37}\text{P}$ , observed in binary grazing reactions, may be described in terms of the coupling of a  $2s_{1/2}$  or  $1d_{3/2}$  proton to the  $J^\pi = 2^+, 4^+, 6^+$  states of  $^{36}\text{Si}$  [5]; in this particular case the core-coupled components correspond to 25%–80% of the total wave function. More recently, as also noted earlier, it has been proposed by Bastin *et al.* [21] that the coupling of either a  $2s_{1/2}$  or  $1d_{3/2}$  proton to the  $2_1^+$  state in  $^{40,42}\text{Si}$  produces states in their  $^{41,43}\text{P}$  isotones, which further supports evidence for the disappearance of the  $N = 28$  spherical gap in this region.

### C. $^{36}\text{P}$

Figure 8 shows sections of a spectrum of  $\gamma$  rays detected in coincidence with the  $Z = 15$ ,  $A = 36$  reaction products detected at the PRISMA focal plane. The observed  $\gamma$  rays associated with the deexcitation of states of  $^{36}\text{P}$  have an uncertainty in  $\gamma$ -ray energy of about  $\pm 1$  keV and are listed in Table I together with their measured relative intensities. The construction of a level scheme for  $^{36}\text{P}$  was informed by  $\gamma$ -ray energy sums and intensities and by the results of previous experimental studies [51,52,56–58].

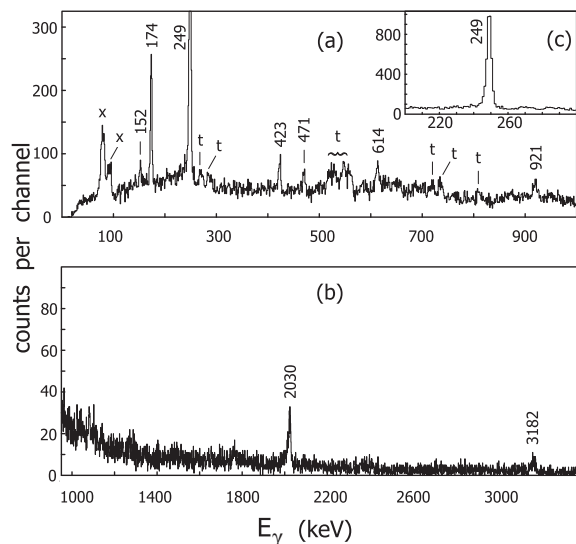


FIG. 8. Sections of the spectrum of  $\gamma$  rays, in the energy range (a) to 1 MeV and (b) from 1 to 3.4 MeV, detected in coincidence with the  $Z = 15$ ,  $A = 36$  reaction products identified at the PRISMA focal plane. Panel (c) shows the 249-keV photopeak.

Figure 9 shows the  $^{36}\text{P}$  level scheme of the present work together with those from previously published work [52,56] and from the compilation and evaluations of Endt [57,58]. A recent Nuclear Data Sheets for  $A = 36$  [59] also summarizes the currently available information on the level structure. The results for the negative-parity states of this  $N = 21$  isotone, obtained using the PSDPF shell-model interaction, are also presented. Nine  $\gamma$  rays associated with the deexcitation of  $^{36}\text{P}$  were observed in the present work. Four of these were previously reported [51,57] from a  $\beta$ -decay study of  $^{36}\text{Si}$ .  $\gamma$ -ray transitions of energy 878.2, 934.7, 977.9, 1053.2, and 1856.0 keV, observed by Dufour *et al.* [51,57], have not been observed in the present work. This is perhaps not surprising, because these transitions depopulate states with  $J^\pi$  assignments of  $1^+$ ; as mentioned earlier, quasielastic binary transfer reactions preferentially populate yrast and near-yrast states of the final nucleus. None of the  $^{36}\text{P}$   $\gamma$  rays observed in the present work could be identified in the  $\gamma$ -ray triples data from the  $^{36}\text{S}$  on  $^{176}\text{Yb}$  deep-inelastic experiment [39], to which reference has been made earlier. It is interesting to note that for the  $N = 21$  isotones,  $^{38}\text{Cl}$  [23] and  $^{37}\text{S}$  [54,60], which were also studied in the same PRISMA plus CLARA experiment, the observed  $\gamma$  rays could also not be identified in the thick-target  $\gamma$ -ray triples data. This may be related to the lifetimes of the decaying states; in deep-inelastic measurements with thick targets, transitions are generally observed only when the effective lifetime of the decaying state is longer than the slowing-down time of the recoiling nucleus in the thick target ( $\approx 1$  ps). As discussed below, we have tentatively assigned three of the five previously unreported transitions to the  $^{36}\text{P}$  level scheme.

From a  $\beta$ -decay study of  $^{36}\text{P}$ , the ground state  $J^\pi$  value has been determined to be  $4^-$  [58]; in terms of the simple shell model, this corresponds to the coupling of the unpaired  $2s_{1/2}$

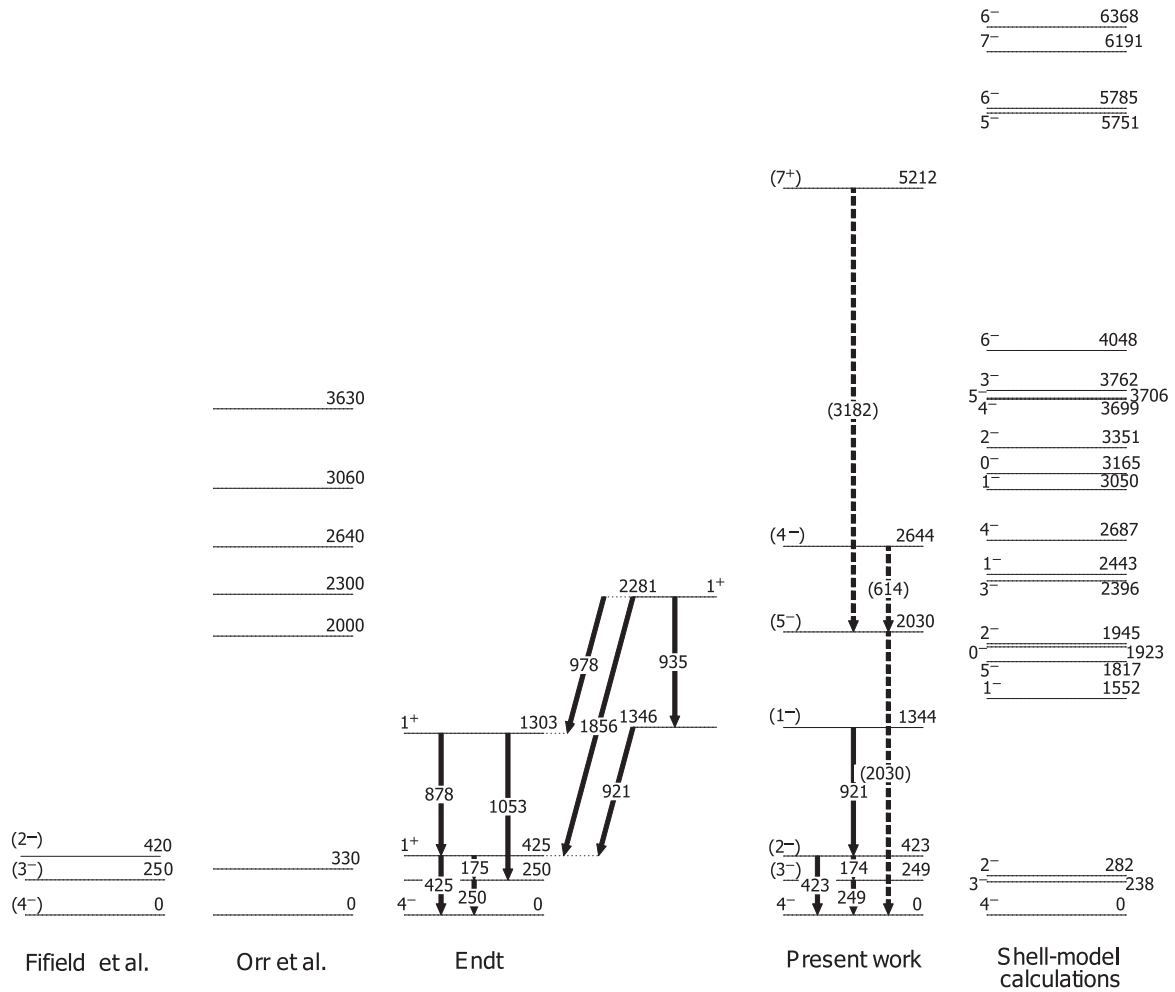


FIG. 9.  $^{36}\text{P}$  level schemes of previous work [52,56–58] and the present work. Also shown are the results shell-model calculations of the negative-parity states for this nucleus based on the PSDPF interaction.

proton to the unpaired  $1f_{7/2}$  neutron. The first excited state of  $^{36}\text{P}$  at 249 keV is strongly populated in the present work. Drumm *et al.* [61], and subsequently Fiffield *et al.* [56], have proposed that this state has a  $J^\pi$  value of  $3^-$ ; it most likely corresponds to the second member of the  $\pi(2s_{1/2}) \otimes \nu(1f_{7/2})$  doublet, because it is populated in the charge-exchange reaction  $^{36}\text{S}(^7\text{Li}, ^7\text{Be})^{36}\text{P}$  [56,61], and the  $^{36}\text{S}$  ground state, on a simple shell-model basis, has two protons in the  $2s_{1/2}$  shell and a vacant  $1f_{7/2}$  neutron shell. Indeed, it is expected that the low-lying levels of  $^{36}\text{P}$  will be described in terms of the coupling of an odd proton in the  $2s_{1/2}$  or  $1d_{3/2}$  shells with an odd neutron, either in the  $1f_{7/2}$  shell or in the  $2p_{3/2}$  shell. The extent to which this simple description is valid will be examined later in the paper when the shell-model wave functions are discussed. The 423-keV state was assigned a  $J^\pi$  value of  $1^+$  by Endt [57], but this is in disagreement with the work of Fiffield *et al.* [56], in which a  $J^\pi$  value of  $2^-$  was proposed. The present work supports the assignment of Fiffield. If the 423-keV state has a  $J^\pi$  value of  $1^+$ , it will decay to the ground state by an  $E3$   $\gamma$ -ray transition and to the 249-keV state by an  $M2$  transition. On this basis, the lifetime of the state would be so long that, in the present experiment, the

excited  $^{36}\text{P}$  nuclei would have exited the PRISMA scattering chamber and the deexcitation  $\gamma$  rays would not be observed experimentally. The 1344-keV excited state was previously reported by Endt [57]; no  $J^\pi$  assignment was proposed. On the basis of an association with the shell-model state at 1552 keV (discussed later), we very tentatively propose a  $J^\pi$  value of  $1^-$ .

Intensity-balance arguments indicate that the 2030-keV  $\gamma$ -ray transition is too intense to be assigned to the direct feeding of either the 423- or 1344-keV excited states. However, it is unlikely that this transition feeds directly into the first excited state at 249 keV; this would require the observation of an excited state at about 2280 keV. Endt [57] reported the observation of an excited state at 2281 keV; however, none of the  $\gamma$  rays reported [57] to decay from this state were observed in the present work. It is therefore tentatively proposed here that the 2030-keV  $\gamma$ -ray transition feeds directly to the ground state. This proposed assignment is consistent, within experimental uncertainties, with the work of Orr *et al.* [52], in which an excited state of  $^{36}\text{P}$  was observed at 2000 keV in a multinucleon transfer reaction,  $^{37}\text{Cl}(^{13}\text{C}, ^{14}\text{O})^{36}\text{P}$ , with an energy resolution of 230 keV (FWHM). Comparison with

the results of an  $0\hbar\omega$  shell-model calculation suggested that the state is the  $J^\pi = 5^-$  member of the  $\pi(d_{3/2}) \otimes \nu(f_{7/2})$  multiplet.

The previously unobserved 614- and 3182-keV  $\gamma$ -ray transitions have been tentatively assigned to the feeding of the 2030-keV excited state. The 614-keV transition may be attributed to the deexcitation of the previously reported [52] 2640(30)-keV excited state, measured here at 2644 keV, while the 3182-keV  $\gamma$  ray may correspond to the decay of a 5212-keV ( $J^\pi = 7^+$ ) stretched state with configuration  $\pi(1f_{7/2}) \otimes \nu(1f_{7/2})$ , predicted by Ollier *et al.* [26], from the systematics of  $J^\pi = 4^-, 5^-,$  and  $7^+$  states in even- $A$  phosphorus isotopes, to be at an energy of approximately 4.8 MeV. Because the state corresponds to the promotion of the odd proton across the  $Z = 20$  shell gap, it lies outside the configuration space of the present  $0\hbar\omega$  shell-model calculations. No spin assignments have previously been proposed for the 2644-keV state; here, on the basis of the  $\gamma$ -ray decay to the 2030-keV  $J^\pi = (5^-)$  state, the feeding characteristics of binary grazing reactions, and comparison with the results of shell-model calculations (see below), we very tentatively propose a  $J^\pi$  value of ( $4^-$ ).

Shell-model calculations, based on the PSDPF interaction, indeed show that the  $J^\pi = 4^-$  and  $3^-$  members of the doublet (ground state and 249-keV excited state) have a configuration dominated,  $\sim 75\%$  and  $\sim 70\%$ , respectively, by the coupling of the unpaired  $2s_{1/2}$  proton to the unpaired  $1f_{7/2}$  neutron. The  $J^\pi = 2^-$  and  $1^-$  states at predicted excitation energies of 282 and 1552 keV, respectively, correspond to the coupling of a  $2s_{1/2}$  proton and a  $2p_{3/2}$  neutron, with contributions of 56% and 75%, respectively, to the total wave function of the states. We propose here that the experimental counterpart of the 282-keV state is that at 423 keV, while the state observed at 1344 keV is the counterpart of the 1552-keV shell-model state. In a simple shell-model picture, the coupling of an unpaired  $1d_{3/2}$  proton to an unpaired  $1f_{7/2}$  neutron gives rise to four states, including those with  $J^\pi$  values of  $5^-$  and  $4^-$ . This coupling appears as the dominant component in the wave function, 79% and 70%, respectively, in the shell-model states at 1817 keV ( $J^\pi = 5^-$ ) and 2687 keV ( $J^\pi = 4^-$ ). The states at 2030 and 2644 keV are the experimental counterparts. The shell-model states at 1923 keV ( $J^\pi = 0^-$ ) and at 2443 keV ( $J^\pi = 1^-$ ) have significant components in their wave functions (59% and 38%, respectively) corresponding to the coupling of a  $2s_{1/2}$  proton and a  $2p_{1/2}$  neutron; no experimental counterparts have so far been reported. The coupling of a  $1d_{3/2}$  proton and a  $2p_{3/2}$  neutron results in the cluster of shell-model states at excitation energies of 3050 ( $J^\pi = 1^-$ ), 3165 ( $J^\pi = 0^-$ ), 3351 ( $J^\pi = 2^-$ ), and 3762 keV ( $J^\pi = 3^-$ ); this configuration contributes in the range (38%–66%) to the total wave function. None of these states has, to date, been observed.

We now compare the experimental and shell-model level schemes; see Fig. 9. The  $J^\pi = 1^+$  states at excitation energies of 1303 and 2281 keV are not  $0\hbar\omega$  states and are therefore not included in the present shell-model calculations; they presumably have configurations such as  $\pi(2s_{1/2})^1 \otimes \nu(1d_{3/2})^3(1f_{7/2})^2$ . The structure of all states observed in the present work has been discussed above. It has been

proposed above that the 5212-keV state may correspond to the  $\pi(1f_{7/2})^1 \otimes \nu(1f_{7/2})^1$  ( $J^\pi = 7^+$ ) stretched state. The  $J^\pi = 4^-$  ground state and the 2030-keV  $J^\pi = (5^-)$  state, as noted above, also correspond to stretched configurations in which the unpaired  $1f_{7/2}$  neutron is coupled to the  $2s_{1/2}$  and  $1d_{3/2}$  protons, respectively. As expected, these stretched states are the most strongly bound of the corresponding multiplet of states as a consequence of the larger spatial overlap of the wave functions. The overall agreement between shell model and experiment is good, although it should be borne in mind that the spin assignments made here are tentative.

#### D. $^{37}\text{P}$

As noted earlier, a  $^{37}\text{P}$  level scheme from the present experiment has been published previously by Hodsdon *et al.* [5] and this remains the most recent information on  $^{37}\text{P}$ . The shell-model results presented by Hodsdon correspond to the SDPF-NR effective interaction, first used in the work of Nummela *et al.* [62]. For completeness, the  $^{37}\text{P}$  level scheme is presented here again in Fig. 10 and compared with the results of shell-model calculations based on an improved version of this interaction, namely the SDPF-U interaction of Nowacki and Poves [3]. The SDPF-U effective interaction is composed of three blocks,  $sd$ - $sd$ ,  $sd$ - $pf$ , and  $pf$ - $pf$ ; here, the full  $sd(pf)$  valence space has been used for protons (neutrons) above an  $^{16}\text{O}$  core. The overall agreement between experiment and shell model is very good.

It is of interest to understand the extent to which the low-lying levels correspond to single-particle states, i.e., the occupancy of the  $2s_{1/2}$  and  $1d_{3/2}$  proton shell-model states coupled to an inert neutron core. This is particularly important within the context of discussions of changes to shell structure related to the tensor force. Such discussions normally assume that the states concerned are single-particle states. In reality, the centroid of the single-particle strength is normally not known experimentally. For the  $J^\pi = 1/2^+$  ground state, the configuration  $\pi(1d_{5/2})^6(2s_{1/2})^1(1d_{3/2})^0 \otimes \nu(1d_{5/2})^6(2s_{1/2})^2(1d_{3/2})^4(1f_{7/2})^2$  contributes 55% to the total wave function while the configuration  $\pi(1d_{5/2})^6(2s_{1/2})^1(1d_{3/2})^0 \otimes \nu(0^+)$  contributes 75%. In the latter case, there are configurations of the form  $\pi(1d_{5/2})^6(2s_{1/2})^1(1d_{3/2})^0 \otimes \nu(1d_{5/2})^6(2s_{1/2})^2(1d_{3/2})^4(1f_{7/2})^0(2p_{3/2})^2$ , which involve changes to the configuration of the neutron core. For the  $J^\pi = 3/2^+$  state, there is a significant component in its wave function, 46%, corresponding to the configuration  $\pi(2s_{1/2})^1 \otimes \nu(2^+)$ , and this state cannot be regarded as a pure single-particle state.

#### E. $^{38}\text{P}$

$^{38}\text{P}$  is the most neutron-rich phosphorus isotope populated in the present work and is seven neutrons from stability. There is no information available in the literature on the level structure of this nucleus.

Figure 11 shows the  $\gamma$ -ray spectrum for  $^{38}\text{P}$  from the present work. There is a single  $\gamma$ -ray photopeak at an energy of 380 keV. Another, more weakly defined, photopeak-like

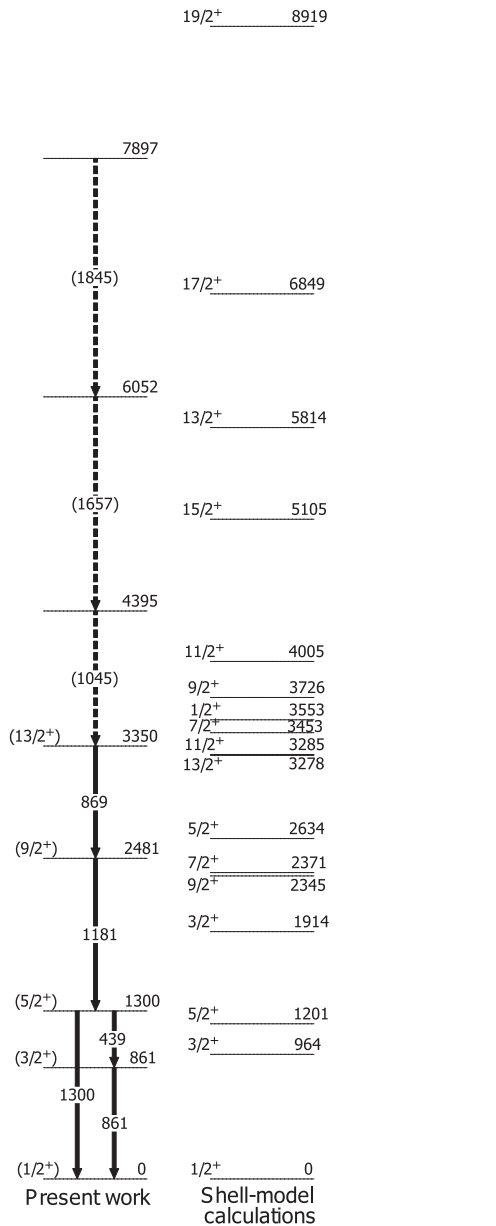


FIG. 10. The  $^{37}\text{P}$  level scheme from the present work and the results of shell-model calculations based on the SDPF-U interaction [3].

structure can be seen at an energy of about 520 keV. However, owing to the low statistics recorded here, it is difficult to conclude that it corresponds to a  $^{38}\text{P}$   $\gamma$ -ray transition. It is

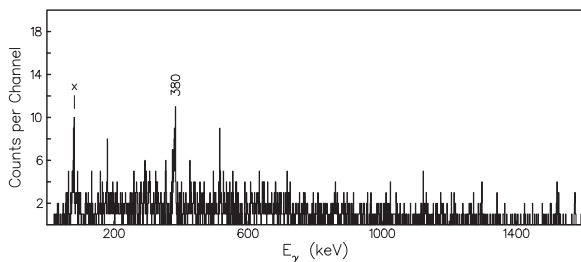


FIG. 11. A spectrum of  $\gamma$  rays detected in coincidence with the  $Z = 15$ ,  $A = 38$  reaction products at the PRISMA focal plane.

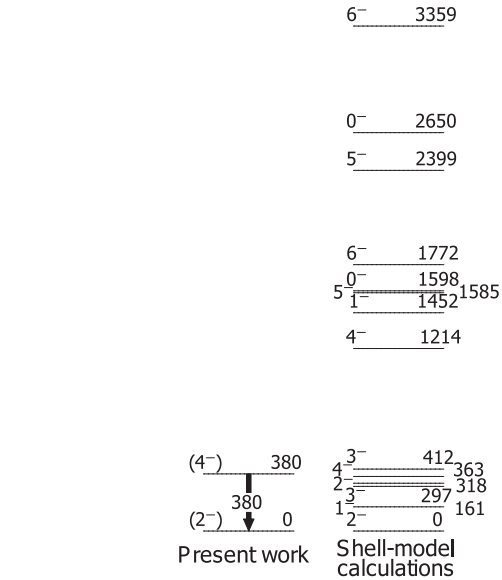


FIG. 12. The  $^{38}\text{P}$  level scheme from the present work, and the results of shell-model calculations, based on the SDPF-U interaction.

proposed here that the 380-keV  $\gamma$  ray corresponds to the depopulation of a low-lying yrast state of  $^{38}\text{P}$ .

Although the  $^{38}\text{P}$  ground-state spin and parity have not been experimentally determined, a limit on its value may be obtained from the results of a  $^{38}\text{P}$   $\beta$ -decay study [51]. The observed feeding of the 1292-keV  $J^\pi = 2^+$  state of  $^{38}\text{S}$  in the  $\beta$  decay of  $^{38}\text{P}$  indicates that the ground state of  $^{38}\text{P}$  has possible  $J^\pi$  values of  $0^-$ ,  $1^-$ ,  $2^-$ ,  $3^-$ , or  $4^-$ . In terms of the simple shell model,  $^{38}\text{P}$  is expected to have a ground-state  $J^\pi$  value of  $4^-$  or  $3^-$  corresponding to the coupling of the unpaired  $2s_{1/2}$  proton with an unpaired  $1f_{7/2}$  neutron. A comparison with  $^{36}\text{P}$ , which has as a ground-state  $J^\pi$  value of  $4^-$ , corresponding to the same proton and neutron coupling, would suggest that the ground and first excited states of  $^{38}\text{P}$  have  $J^\pi$  values of  $4^-$  and  $3^-$ , respectively.

Figure 12 shows the results of shell-model calculations for this nucleus using an SDPF-U interaction, in which the neutrons up to  $N = 20$  are treated as a closed shell and the valence protons and neutrons are confined to the  $sd$  and  $fp$  shells, respectively. The shell model surprisingly predicts a  $^{38}\text{P}$  ground-state  $J^\pi$  value of  $2^-$ . The dominant components of the wave function correspond to  $\pi(1d_{3/2})^1 \otimes \nu(1f_{7/2})^3$  ( $\sim 22\%$ ) and  $\pi(2s_{1/2})^1 \otimes \nu(1f_{7/2})^3$  ( $\sim 21\%$ ). In the ground state of  $^{38}\text{P}$ , the three neutrons which occupy the  $1f_{7/2}$  shell-model orbital couple to  $J^\pi$  values of  $3/2^-$ ,  $5/2^-$ , and  $7/2^-$ , with probabilities of  $\sim 29\%$ ,  $\sim 39\%$ , and  $\sim 26\%$ , respectively. The wave function of the ground state is therefore quite mixed. In the ground states of the  $N = 23$  isotones,  $^{39}\text{S}$  and  $^{37}\text{Si}$ , it has been proposed that the three  $1f_{7/2}$  neutrons are coupled to total angular momentum values of  $(7/2)^-$  [63] and  $7/2^-$  [64], respectively; however, it should be noted that neither spin assignment has been unambiguously made on the basis of experimental measurement. Shell-model calculations based on the SDPF-U interaction give a  $J^\pi$  value of  $7/2^-$  for the ground state of  $^{39}\text{S}$ ; while  $\sim 62\%$  of the wave function corresponds

to neutrons with spin and parity of  $7/2^-$  coupled to protons with a  $J^\pi$  value of  $0^+$ , in only  $\sim 28\%$  of the wave function are three neutrons in the  $1f_{7/2}$  shell coupled to protons with the closed-shell configuration  $\pi(1d_{5/2})^6(2s_{1/2})^2$ . For  $^{37}\text{Si}$ , the shell-model calculations give a ground-state  $J^\pi$  value of  $5/2^-$  and a first excited state at an excitation energy of 170 keV with  $J^\pi$  value of  $7/2^-$ . For the ground state, the largest component ( $\sim 38\%$ ) of the wave function corresponds to three  $1f_{7/2}$  neutrons coupled to an inert  $(1d_{5/2})^6$  proton core.

The lowest-lying  $J^\pi = 3^-$  and  $4^-$  states, which one might naively expect to correspond to the doublet which results from the coupling of a  $1f_{7/2}$  neutron with the unpaired  $2s_{1/2}$  proton, have, within the context of the current shell-model calculations, a structure quite different from such expectations. For the  $3^-$  state, only  $\sim 1\%$  of the wave function corresponds to neutrons with  $J^\pi = 7/2^-$  coupled to protons with  $J^\pi = 1/2^+$ . Although the largest component ( $\sim 36\%$ ) of the wave function corresponds to the configuration  $\pi(2s_{1/2})^1 \otimes \nu(1f_{7/2})^3$ , the three  $1f_{7/2}$  neutrons are coupled mainly to spin  $5/2$ . However, for the  $4^-$  state,  $\sim 63\%$  of the wave function corresponds to neutrons with  $J^\pi = 7/2^-$  coupled to protons with  $J^\pi = 1/2^+$ . Thus, these two states, which in  $^{36}\text{P}$  have very similar structures, are quite dissimilar in  $^{38}\text{P}$  and certainly cannot be considered to be members of a doublet.

We would expect yrast states of  $^{38}\text{P}$  to be populated in the present  $-1p + 3n$  four-nucleon transfer reaction. In relation to the shell-model level scheme of Fig. 12, the experimental counterpart of the  $J^\pi = 4^-$  state at an excitation energy of 363 keV is the lowest-lying excited state which we would expect to be significantly populated. This state will decay to the ground state by an  $E2$  transition and here we propose that this corresponds to the observed transition at an energy of 380 keV; see Fig. 12.

#### F. Structure of first-excited $J^\pi = 1/2^+$ , $3/2^+$ , and $5/2^+$ states of the odd- $A$ P isotopes

It is of interest to examine the shell-model wave functions of the lowest  $J^\pi = 1/2^+$ ,  $3/2^+$ , and  $5/2^+$  states in the sequence of odd- $A$  phosphorus isotopes corresponding to the filling of the neutron  $1f_{7/2}$  shell. For this range of isotopes, the ground-state  $J^\pi$  value is  $1/2^+$ , the first excited state has a  $J^\pi$  value of  $3/2^+$ , and, for the second excited state,  $J^\pi$  is  $5/2^+$ . Within the context of the simple shell model, the lowest-lying  $J^\pi = 1/2^+$  and  $3/2^+$  states correspond to the coupling of a single unpaired proton in the  $2s_{1/2}$  and  $1d_{3/2}$  orbitals, respectively, to an inert even-even  $^{14}\text{Si}$  core, while the lowest-lying  $J^\pi = 5/2^+$  state corresponds to a proton two-particle one-hole configuration,  $\pi(2s_{1/2})^2 \pi(1d_{5/2})^{-1}$ , coupled to the neutron core. Figure 13 presents the results of shell-model calculations of the main components of the wave function of the  $J^\pi = 1/2^+$  ground states of the odd- $A$  phosphorus isotopes. For  $^{35}\text{P}$ , the  $J^\pi = 1/2^+$  ground state is essentially a pure single-proton state, in which an odd  $2s_{1/2}$  proton is coupled to a  $^{34}\text{Si}$  ground-state core. This is not unexpected, because  $^{34}\text{Si}$  has a closed shell of neutrons and a closed  $1d_{5/2}$  proton shell. With increasing neutron number, the wave function of the  $1/2^+$  state becomes more complicated with significant components (12%–39%) corresponding to

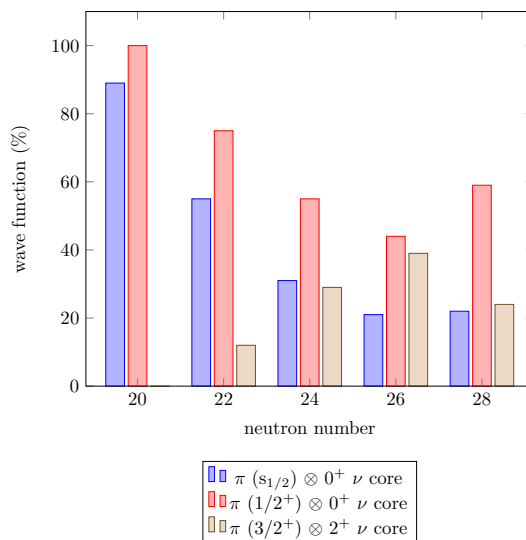


FIG. 13. (Color online) Main wave-function components of the ground state of odd- $A$  phosphorus isotopes.

protons coupled to  $J^\pi = 3/2^+$  and neutrons to  $2^+$ ; see Fig. 13. For protons with  $J^\pi = 1/2^+$  coupled to a  $J^\pi = 0^+$  inert neutron core the contribution from the proton configuration  $\pi(1d_{5/2})^6(2s_{1/2})^1$  becomes as small as 37% for  $N = 28$   $^{43}\text{P}$ , reflecting a more complex coupling of protons to total spin  $1/2^+$ . There is a similar situation in relation to the first  $3/2^+$  state (see Fig. 14); it is a relatively pure single-particle state only for  $^{35}\text{P}$ . The configuration in which protons with  $J^\pi = 1/2^+$  are coupled to neutrons with total spin value  $2^+$  accounts for 10%–46% of the wave function. For neutron number 28, there is a significant difference in the contributions to the wave function from the configurations  $\pi(1d_{3/2})^1 \otimes \nu(0^+)$  (30%)

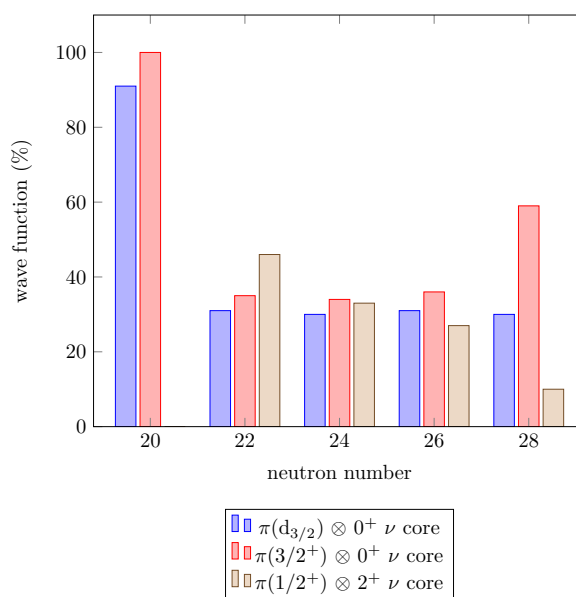


FIG. 14. (Color online) Main wave-function components of the first  $3/2^+$  state of odd- $A$  phosphorus isotopes.

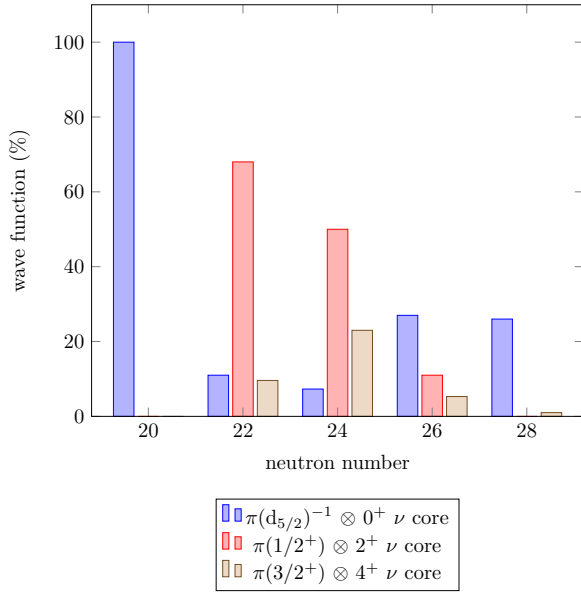


FIG. 15. (Color online) Main wave-function components of the first  $5/2^+$  state of odd-A phosphorus isotopes.

and  $\pi(3/2^+) \otimes \nu(0^+)$  (59%), again reflecting a more complex coupling of proton angular momentum to  $3/2^+$ . For the first  $5/2^+$  state (see Fig. 15), only  $^{35}\text{P}$  has a pure proton two-particle one-hole configuration, as expected. Configurations in which protons are coupled to angular momentum  $1/2^+$  and neutrons to angular momentum  $2^+$  contribute up to 68% of the wave function ( $^{37}\text{P}$ ). Coupling to neutrons with  $J^\pi = 4^+$  makes a small (<25%) contribution to the wave function of the first  $5/2^+$  state.

### G. Evolution of $E(1/2_1^+) - (3/2_1^+)$ binding energy difference for the even-A P isotopes with $20 \leq N \leq 28$ and the associated nuclear collectivity

Figure 16 presents the experimental (red) binding energy difference,  $E(1/2_1^+) - E(3/2_1^+)$ , as a function of neutron number for the odd-A isotopes of phosphorus for neutron numbers in the range from 20 to 28. The energy differences from the results of shell-model calculations (blue), based on the SDPF-U interaction, except for  $^{35}\text{P}$ , where the energy difference is calculated using the PSDPF interaction, are also presented. The agreement between experiment and shell model is good. As has been noted in earlier publications, e.g., Ref. [1], the energy gap between the first  $3/2^+$  and  $1/2^+$  states decreases with increasing neutron number and, for the isotopes of K [9] and Cl [10], an inversion takes place. As also noted earlier, the increase in binding of the  $1d_{3/2}$  proton with respect to the  $2s_{1/2}$  proton with increasing occupation of the  $1f_{7/2}$  neutron shell has been attributed to the monopole component of the tensor interaction. The decrease in energy between the states leads to a pseudo-SU3 symmetry [65], which, in turn, leads to the onset of quadrupole deformation in the adjacent even-A isotopes of S [66,67]. In addition, as neutrons are added to the  $1f_{7/2}$  shell, there is a tendency for the nucleus to adopt a quadrupole deformation to remove the degeneracy

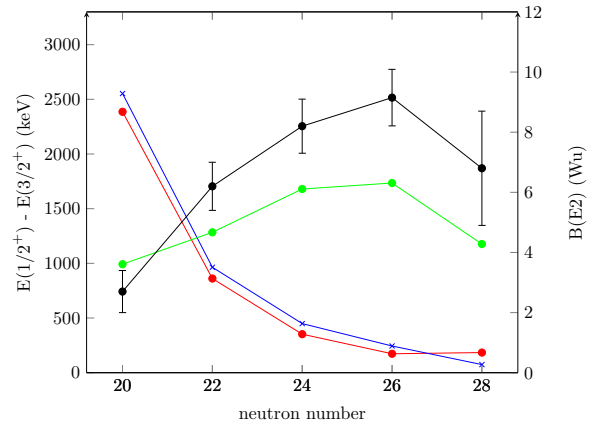


FIG. 16. (Color online) Experimental (red) and shell-model (blue) binding energy difference  $E(1/2_1^+) - E(3/2_1^+)$ , as a function of neutron number for the odd-A isotopes of phosphorus. Shell-model  $B(E2)$  values corresponding to the transition  $3/2^+ \rightarrow 1/2^+$  (green) and experimental  $B(E2)$  values in Weisskopf units for the  $2^+ \rightarrow 0^+$  transitions in the even-A sulfur isotones (black) are also shown. See text for details.

associated with the increasing occupancy of the  $1f_{7/2}$  shell. This is the nuclear analog of the Jahn-Teller effect [68,69]; this effect was first discussed in 1937 in relation to the stability of polyatomic molecules in degenerate electronic states [70]. Figure 16 also presents  $B(E2; 2^+ \rightarrow 0^+)$  values (black) for the even-A isotopes of sulfur, from the work of Scheit *et al.* [66] and of Glasmacher *et al.* [67]. It can be seen that there is an increase in collectivity with increasing neutron number. The collectivity reaches a maximum at  $N = 26$   $^{42}\text{S}$ . The drop in  $B(E2)$  value at  $N = 28$  is related to neutron shell-closure effects; it is also known that there is shape coexistence in the neutron-rich sulfur isotope,  $^{44}\text{S}$  [71,72]. Shell-model  $B(E2)$  values corresponding to the transition  $3/2^+ \rightarrow 1/2^+$  between the two lowest states of the isotopes of phosphorus are also presented in Fig. 16. In the calculation of  $E2$  electromagnetic transition probabilities, effective charges of  $e_{\text{eff}}(p) = 1.36e$  and  $e_{\text{eff}}(n) = 0.45e$  were used [73]. It is interesting to note that the dependence of  $B(E2)$  values on neutron number is very similar to that of the experimental  $B(E2; 2^+ \rightarrow 0^+)$  values for the even-A isotopes of sulphur. It would also be instructive to compare the  $B(E2)$  values with those of the even-A Si isotones, because one may consider, as discussed earlier, the odd-A phosphorus isotopes to correspond to an odd proton coupled to an even-A silicon core. However, the  $B(E2; 2^+ \rightarrow 0^+)$  values for the neutron-rich even-A silicon isotopes have been measured only for neutron numbers up to 24 [74]. There has been one measurement of  $B(E2; 3/2^+ \rightarrow 1/2^+)$  for the odd-A isotopes of phosphorus, namely that of Ibbotson *et al.* [75] for  $^{39}\text{P}$ . The experimental value,  $B(E2; 3/2^+ \rightarrow 1/2^+) = 49 \pm 15 e^2 \text{fm}^4$  agrees very well with the shell-model value of  $58 e^2 \text{fm}^4$ . Confirmation, or otherwise, of agreement between experimental and shell-model  $B(E2)$  values for the other odd-A isotopes of phosphorus, presented in Fig. 16, would be instructive.

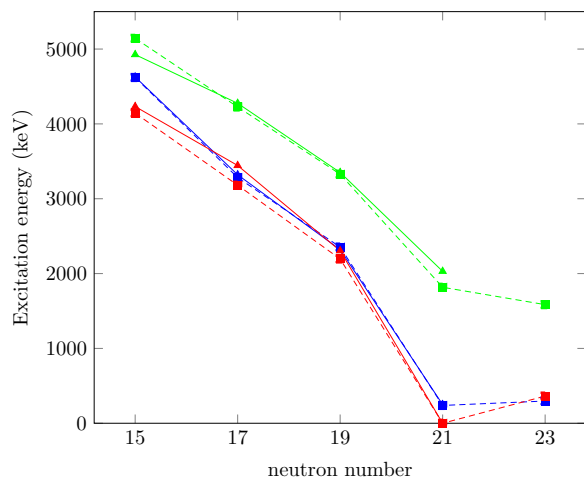


FIG. 17. (Color online) Experimental (triangles, solid lines) and shell-model (squares, dashed lines) excitation energies of the yrast  $3^-$  (blue),  $4^-$  (red), and  $5^-$  (green) states of the even- $A$  phosphorus isotopes as a function of neutron number. (See text for details.)

#### H. The negative-parity, $J^\pi = 3^-, 4^-$ , and $5^-$ states of the even- $A$ P isotopes

In an earlier publication [26], intruder states with stretched configurations  $\pi(2s_{1/2}) \otimes \nu(1f_{7/2})$ ,  $\pi(1d_{3/2}) \otimes \nu(1f_{7/2})$ , and  $\pi(1f_{7/2}) \otimes \nu(1f_{7/2})$  were discussed within the context of the Bansall-French model [76] and a linear dependence of  $np$ -separation energy,  $S(np)$ , for the states with  $J^\pi$  values of  $4^-$ ,  $5^-$ , and  $7^+$ , was observed as a function of mass number, in the range from  $A = 30$  to  $36$ . Here the excitation energies and wave functions of these states will be discussed within the context of state-of-the-art shell-model calculations. The model space used here does not allow a discussion of the  $7^+$  state, because this involves the promotion of a proton across the  $N = 20$  shell gap. However, the discussion will include the  $J^\pi = 3^-$  state which, within a simple shell-model picture, is the non-stretched member of the  $\pi(2s_{1/2}) \otimes \nu(1f_{7/2})$  doublet.

Figures 17 and Fig. 18 present the excitation energies and the main components of the wave functions, respectively, of the yrast  $3^-$ ,  $4^-$ , and  $5^-$  states as a function of neutron number in the range  $15 \leq N \leq 23$ . In Fig. 17, both experimental and shell-model energies are shown. As may be seen, there is excellent agreement between experiment and shell model.

In contrast to the simple shell-model description of these states, it is only for the  $N = 21$ , closed-shell plus one-neutron isotope,  $^{36}\text{P}$ , that the wave functions have, as the dominant component (70%–80%),  $\pi(2s_{1/2}) \otimes \nu(1f_{7/2})$  for the  $J^\pi = 3^-$  and  $4^-$  states and  $\pi(1d_{3/2}) \otimes \nu(1f_{7/2})$  for the  $5^-$  state. The evolution of the wave functions with increasing neutron number is very similar for the  $J^\pi = 3^-$ ,  $4^-$ , and  $5^-$  states in that the contribution of the component  $\pi(2s_{1/2}) \otimes \nu(1f_{7/2})$  to the total wave function for the  $3^-$  and  $4^-$  states [and  $\pi(1d_{3/2}) \otimes \nu(1f_{7/2})$  for the  $5^-$  state] increases from a few percent at  $N = 15$  to about 70%–80% at  $N = 21$ . For the  $N = 23$  isotope,  $^{38}\text{P}$ , the largest wave-function component (63%) of the  $J^\pi = 3^-$  state corresponds to  $\nu(5/2^-)$  coupled to  $\pi(1/2^+)$ . It is interesting to note again that the ground-state  $J^\pi$

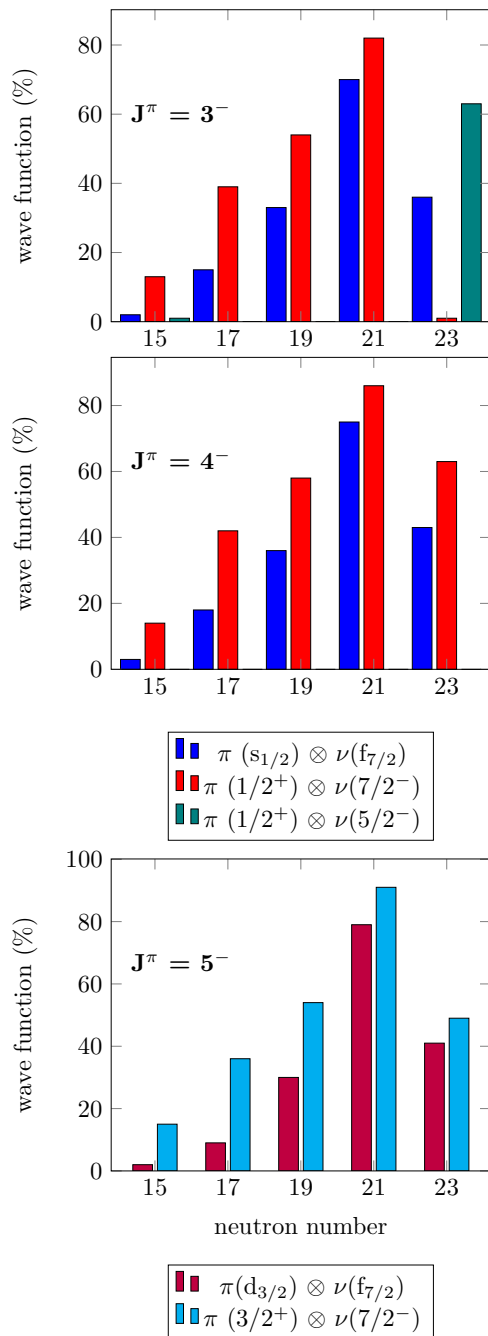


FIG. 18. (Color online) Main wave-function components of the first  $J^\pi = 3^-, 4^-$ , and  $5^-$  states of even- $A$  phosphorus isotopes.

value for the  $N = 23$  isotope  $^{37}\text{Si}$  is predicted, in shell-model calculations based on the SDPF-U effective interaction, to be  $5/2^-$ . For the  $N = 23$  isotope,  $^{39}\text{S}$ , the first excited state, with a predicted  $J^\pi$  value of  $5/2^-$  lies only 72 keV above the  $7/2^-$  ground state. The lowering of the  $(j - 1)$  state relative to the  $j$  state in  $j^3$  configurations was discussed within the context of effective interactions by Talmi [77] in 1962. It is perhaps surprising that, with the rapidly changing contributions to the wave functions of the simple shell-model configuration of core plus extracore  $\nu$ - $\pi$  pair, the systematic behavior of  $np$

separation energy as a function of neutron number, illustrated in the work of Ollier *et al.* [26], holds so remarkably well.

#### IV. SUMMARY

The neutron-rich nuclei  $^{34,35,36,37,38}\text{P}$  were successfully populated via binary grazing reactions using a beam of  $^{36}\text{S}$  ions at 215 MeV on a thin  $^{208}\text{Pb}$  target. The PRISMA magnetic spectrometer in conjunction with the CLARA Ge array at the INFN Legnaro National Laboratory, Italy, were used to identify the isotope and its associated deexcitation  $\gamma$  rays. Level schemes for these nuclei were constructed using a combination of  $\gamma$ -ray energy sums and relative intensity measurements and, where possible, these decay schemes are supported by  $\gamma$ - $\gamma$  coincidence measurements using data obtained in an early thick-target deep-inelastic experiment. The level schemes have been compared with the results of the state-of-the-art shell-model calculations and good agreement is obtained. For the  $N = 21$  nucleus,  $^{36}\text{P}$ , a number of

proposed new spin and parity assignments have been made. The evolution of the energy spacing of the first  $J^\pi = 1/2^+$  and  $3/2^+$  states of the even- $A$  isotopes of phosphorus and its relationship to the associated nuclear collectivity is also discussed. Finally, the evolution with neutron number of the wave functions of the  $J^\pi = 1/2^+$ ,  $3/2^+$ , and  $5/2^+$  states of the odd- $A$  P isotopes and the first  $J^\pi = 3^-, 4^-$ , and  $5^-$  states of the even- $A$  P isotopes is discussed.

#### ACKNOWLEDGMENTS

We would like to thank the technical staff of the INFN Legnaro National Laboratory for their support during this experiment. This work was supported by the EPSRC (U.K.). Four of us (A.H., M.B., K.L.K., and A.P.) would like to acknowledge the receipt of financial support from EPSRC during the course of this work. A.J. would like to acknowledge support from the Spanish Ministerio de Ciencia e Innovación under Contract No. FPA2011-29854-C04. Z.D. acknowledges the financial support from OTKA Grant No. K100835.

- 
- [1] A. Gade, B. A. Brown, D. Bazin, C. M. Campbell, J. A. Church, D. C. Dinca, J. Enders, T. Glasmacher, M. Horoi, Z. Hu, K. W. Kemper, W. F. Mueller, T. Otsuka, L. A. Riley, B. T. Roeder, T. Suzuki, J. R. Terry, K. L. Yurkewicz, and H. Zwahlen, *Phys. Rev. C* **74**, 034322 (2006).
- [2] T. Otsuka, T. Suzuki, R. Fujimoto, H. Grawe, and Y. Akaishi, *Phys. Rev. Lett.* **95**, 232502 (2005).
- [3] F. Nowacki and A. Poves, *Phys. Rev. C* **79**, 014310 (2009).
- [4] S. Khan, Th. Khim, K. T. Knöpfle, G. Mairle, V. Bechtold, and L. Friedrich, *Phys. Lett. B* **156**, 155 (1985).
- [5] A. Hodsdon *et al.*, *Phys. Rev. C* **75**, 034313 (2007).
- [6] P. Doll, G. J. Wagner, K. T. Knöpfle, and G. Mairle, *Nucl. Phys. A* **263**, 210 (1976).
- [7] S. M. Banks, B. M. Spicer, G. G. Shute, V. C. Officer, G. J. Wagner, W. E. Dollhopf, L. I. Qingli, C. W. Glover, D. W. Devins, and D. L. Friesel, *Nucl. Phys. A* **437**, 381 (1985).
- [8] O. Sorlin and M.-G. Porquet, *Prog. Part. Nucl. Phys.* **61**, 602 (2008).
- [9] J. H. Bjerregaard, O. Hansen, O. Nathan, R. Stock, R. Chapman, and S. Hinds, *Phys. Lett. B* **24**, 568 (1967).
- [10] X. Liang, R. Chapman, F. Haas, K.-M. Spohr, P. Bednarczyk, S. M. Campbell, P. J. Dagnall, M. Davison, G. de Angelis, G. Duchêne, Th. Kröll, S. Lunardi, S. Naguleswaran, and M. B. Smith, *Phys. Rev. C* **66**, 037301 (2002).
- [11] O. Sorlin *et al.*, *Eur. Phys. J. A* **22**, 173 (2004).
- [12] C. Thibault, R. Klapisch, C. Rigaud, A. M. Poskanzer, R. Prieels, L. Lessard, and W. Reisdorf, *Phys. Rev. C* **12**, 644 (1975).
- [13] C. Détraz, D. Guillemaud, G. Huber, R. Klapisch, M. Langevin, F. Naulin, C. Thibault, L. C. Carraz, and F. Touchard, *Phys. Rev. C* **19**, 164 (1979).
- [14] D. Guillemaud-Mueller, C. Détraz, M. Langevin, F. Naulin, M. de Saint-Simon, C. Thibault, F. Touchard, and M. Epherre, *Nucl. Phys. A* **426**, 37 (1984).
- [15] T. Motobayashi, Y. Ikeda, Y. Ando, K. Ieki, M. Inoue, N. Iwasa, T. Kikuchi, M. Kurokawa, S. Moriya, S. Ogawa, H. Murakami, S. Shimoura, Y. Yanagisawa, T. Nakamura, Y. Watanabe, M. Ishihara, T. Teranishi, H. Okuno, and R. F. Casten, *Phys. Lett. B* **346**, 9 (1995).
- [16] B. V. Pritychenko, T. Glasmacher, P. D. Cottle, M. Fauerbach, R. W. Ibbotson, K. W. Kemper, V. Maddalena, A. Navin, R. Ronningen, A. Sakharuk, H. Scheit, and V. G. Zelevinsky, *Phys. Lett. B* **461**, 322 (1999).
- [17] V. Chiste *et al.*, *Phys. Lett. B* **514**, 233 (2001).
- [18] B. J. Cole, A. Watt, and R. R. Whitehead, *J. Phys. A* **7**, 1374 (1974).
- [19] A. Poves and J. Retamosa, *Phys. Lett. B* **184**, 311 (1987).
- [20] X. Liang *et al.*, *Phys. Rev. C* **74**, 014311 (2006).
- [21] B. Bastin *et al.*, *Phys. Rev. Lett.* **99**, 022503 (2007).
- [22] Z. M. Wang *et al.*, *Phys. Rev. C* **81**, 054305 (2010).
- [23] D. O'Donnell *et al.*, *Phys. Rev. C* **81**, 024318 (2010).
- [24] Z. M. Wang *et al.*, *Phys. Rev. C* **81**, 064301 (2010).
- [25] Z. M. Wang *et al.*, *Phys. Rev. C* **83**, 061304(R) (2011).
- [26] J. Ollier, R. Chapman, X. Liang, M. Labiche, K.-M. Spohr, M. Davison, G. de Angelis, M. Axiotis, T. Kröll, D. R. Napoli, T. Martinez, D. Bazzacco, E. Farnea, S. Lunardi, A. G. Smith, and F. Haas, *Phys. Rev. C* **71**, 034316 (2005).
- [27] X. Liang, R. Chapman, F. Haas, K. M. Spohr, P. Bednarczyk, S. M. Campbell, P. J. Dagnall, M. Davison, G. de Angelis, G. Duchêne, Th. Kröll, S. Lunardi, S. Naguleswaran, and M. B. Smith, *Phys. Rev. C* **66**, 014302 (2002).
- [28] J. Ollier, R. Chapman, X. Liang, M. Labiche, K. M. Spohr, M. Davison, G. de Angelis, M. Axiotis, T. Kröll, D. R. Napoli, T. Martinez, D. Bazzacco, E. Farnea, S. Lunardi, and A. G. Smith, *Phys. Rev. C* **67**, 024302 (2003).
- [29] E. Caurier and F. Nowacki, *Acta. Phys. Pol. B* **30**, 705 (1999).
- [30] E. Caurier, G. Martínez-Pinedo, F. Nowacki, A. Poves, J. Retamosa, and A. P. Zuker, *Phys. Rev. C* **59**, 2033 (1999).
- [31] A. M. Stefanini, L. Corradi, G. Maron, A. Pisent, M. Trotta, A. M. Vinodkumar, S. Beghini, G. Montagnoli, F. Scarlassara, G. F. Segato, A. De Rosa, G. Inglima, D. Pierroutsakou, M. Romoli, M. Sandoli, G. Pollarolo, and A. Latina, *Nucl. Phys. A* **701**, 217c (2002).



- [32] G. Montagnoli *et al.*, *Nucl. Instrum. Methods Phys. Res. A* **547**, 455 (2005).
- [33] S. Beghini, L. Corradi, E. Fioretto, A. Gadea, A. Latina, G. Montagnoli, F. Scarlassara, A. M. Stefanini, S. Szilner, M. Trotta, and A. M. Vinodkumar, *Nucl. Instrum. Methods Phys. Res. A* **551**, 364 (2005).
- [34] A. Gadea (EUROBALL Collaboration and PRISMA-2 collaboration), *Eur. Phys. J. A* **20**, 193 (2004).
- [35] M. W. Guidry, S. Juutinen, X. T. Liu, C. R. Bingham, A. J. Larabee, L. L. Riedinger, C. Baktash, I. Y. Lee, M. L. Halbert, D. Cline, B. Kotlinski, W. J. Kernan, T. M. Semkow, D. G. Sarantites, K. Honkanen, and M. Rajagopalan, *Phys. Lett. B* **163**, 79 (1985).
- [36] H. Takai, C. N. Knott, D. F. Winchell, J. X. Saladin, M. S. Kaplan, L. de Faro, R. Aryaenejad, R. A. Blue, R. M. Ronningen, D. J. Morrissey, I. Y. Lee, and O. Dietzsch, *Phys. Rev. C* **38**, 1247 (1988).
- [37] B. Fornal, R. H. Mayer, I. G. Bearden, Ph. Benet, R. Broda, P. J. Daly, Z. W. Grabowski, I. Ahmad, M. P. Carpenter, P. B. Fernandez, R. V. F. Janssens, T. L. Khoo, T. Lauritsen, E. F. Moore, and M. Drigert, *Phys. Rev. C* **49**, 2413 (1994).
- [38] J. F. C. Cocks *et al.*, *Nucl. Phys. A* **645**, 61 (1999).
- [39] J. Ollier, Ph.D. thesis, University of Paisley (2004).
- [40] P. C. Bender *et al.*, *Phys. Rev. C* **80**, 014302 (2009).
- [41] P. C. Bender *et al.*, *Phys. Rev. C* **85**, 044305 (2012).
- [42] R. Chakrabarti, S. Mukhopadhyay, Krishichayan, A. Chakraborty, A. Ghosh, S. Ray, S. S. Ghugre, A. K. Sinha, L. Chaturvedi, A. Y. Deo, I. Mazumdar, P. K. Joshi, R. Palit, Z. Naik, S. Kumar, N. Madhavan, R. P. Singh, S. Muralithar, B. K. Yogi, and U. Garg, *Phys. Rev. C* **80**, 034326 (2009).
- [43] P. J. R. Mason *et al.*, *Phys. Rev. C* **85**, 064303 (2012).
- [44] A. M. Nathan and D. E. Alburger, *Phys. Rev. C* **15**, 1448 (1977).
- [45] A. Krishichayan *et al.*, *Eur. Phys. J. A* **29**, 151 (2006).
- [46] F. Ajzenberg-Selove, E. R. Flynn, S. Orbesen, and J. W. Sunier, *Phys. Rev. C* **15**, 1 (1977).
- [47] M. Asai, T. Ishii, A. Makishima, M. Ogawa, and M. Matsuda, in *Proceedings of the Third International Conference on Fission and Properties of Neutron-Rich Nuclei*, edited by J. H. Hamilton, A. V. Ramayya, and H. K. Carter (World Scientific, Singapore, 2002), pp. 259–265.
- [48] M. Bouhelal, F. Haas, E. Caurier, F. Nowacki, and A. Bouldjedri, *Nucl. Phys. A* **864**, 113 (2011).
- [49] B. A. Brown and W. A. Richter, *Phys. Rev. C* **74**, 034315 (2006).
- [50] C. E. Thorn, J. W. Olness, E. K. Warburton, and S. Raman, *Phys. Rev. C* **30**, 1442 (1984).
- [51] J. P. Dufour, R. Del Moral, A. Fleury, F. Hubert, D. Jean, M. S. Pravikoff, H. Delagrange, H. Geissel, and K.-H. Schmidt, *Z. Phys. A* **324**, 487 (1986).
- [52] N. A. Orr, W. N. Catford, L. K. Fifield, T. R. Ophel, D. C. Weisser, and C. L. Woods, *Nucl. Phys. A* **477**, 523 (1988).
- [53] M. Wiedeking *et al.*, *Phys. Rev. C* **78**, 037302 (2008).
- [54] Z. M. Wang, Ph.D. thesis, University of the West of Scotland (2010).
- [55] M. Bouhelal, F. Haas, E. Caurier, and F. Nowacki, *AIP Conf. Proc.* **1491**, 38 (2012).
- [56] L. K. Fifield, W. N. Catford, N. A. Orr, T. R. Ophel, A. Etchegoyen, and M. C. Etchegoyen, *Nucl. Phys. A* **552**, 125 (1993).
- [57] P. M. Endt, *Nucl. Phys. A* **521**, 1 (1990).
- [58] P. M. Endt, *Nucl. Phys. A* **633**, 1 (1998).
- [59] N. Nica, J. Cameron, and B. Singh, *Nuclear Data Sheets* **113**, 1 (2012).
- [60] Z. M. Wang *et al.* (unpublished).
- [61] P. V. Drumm, L. K. Fifield, R. A. Bark, M. A. C. Hotchkis, C. L. Woods, and P. Maier-Komor, *Nucl. Phys. A* **441**, 95 (1985).
- [62] S. Nummela, P. Baumann, E. Caurier, P. Dessagne, A. Jokinen, A. Knipper, G. Le Scornet, C. Miehé, F. Nowacki, M. Oinonen, Z. Radivojevic, M. Ramdhane, G. Walter, J. Äystö, and the ISOLDE Collaboration, *Phys. Rev. C* **63**, 044316 (2001).
- [63] B. Singh and J. A. Cameron, *Nuclear Data Sheets* **107**, 225 (2006).
- [64] J. A. Cameron, J. Chen, and B. Singh, *Nuclear Data Sheets* **113**, 365 (2012).
- [65] J. Retamosa, E. Caurier, F. Nowacki, and A. Poves, *Phys. Rev. C* **55**, 1266 (1997).
- [66] H. Scheit, T. Glasmacher, B. A. Brown, J. A. Brown, P. D. Cottle, P. G. Hansen, R. Harkewicz, M. Hellström, R. W. Ibbotson, J. K. Jewell, K. W. Kemper, D. J. Morrissey, M. Steiner, P. Thirolf, and M. Thoennessen, *Phys. Rev. Lett.* **77**, 3967 (1996).
- [67] T. Glasmacher, B. A. Brown, M. J. Chromik, P. D. Cottle, M. Fauerbach, R. W. Ibbotson, K. W. Kemper, D. J. Morrissey, H. Scheit, D. W. Sklenicka, and M. Steiner, *Phys. Lett. B* **395**, 163 (1997).
- [68] P. G. Reinhard and E. W. Otten, *Nucl. Phys. A* **420**, 173 (1984).
- [69] W. Nazarewicz, *Nucl. Phys. A* **574**, 27c (1994).
- [70] H. A. Jahn and E. Teller, *Proc. R. Soc. London. A* **161**, 220 (1937).
- [71] S. Grévy *et al.*, *Eur. Phys. J. A* **25**, 111 (2005).
- [72] C. Force *et al.*, *Phys. Rev. Lett.* **105**, 102501 (2010).
- [73] W. A. Richter, S. Mkhize, and B. A. Brown, *Phys. Rev. C* **78**, 064302 (2008).
- [74] R. W. Ibbotson, T. Glasmacher, B. A. Brown, L. Chen, M. J. Chromik, P. D. Cottle, M. Fauerbach, K. W. Kemper, D. J. Morrissey, H. Scheit, and M. Thoennessen, *Phys. Rev. Lett.* **80**, 2081 (1998).
- [75] R. W. Ibbotson, T. Glasmacher, P. F. Mantica, and H. Scheit, *Phys. Rev. C* **59**, 642 (1999).
- [76] R. K. Bansal and J. B. French, *Phys. Lett.* **11**, 145 (1964).
- [77] I. Talmi, *Rev. Mod. Phys.* **34**, 704 (1962).